

**Interactive comment on “Projected sea level rise and changes in extreme storm surge and wave events during the 21st century in the region of Singapore” by H. Cannaby et al.**

We thank the reviewers for their constructive comments on our paper. Responses to each individual comment are included below (in red text for clarity). The revised text showing tracked changes follows the response.

**Response to comments from reviewer #1**

I would encourage the authors to compare their sea-level rise projections to other published projections for Singapore, such as those generated by Kopp et al. 2014 (doi:10.1002/2014EF000239) as part of their global set of tide-gauge-specific sea-level rise projections. Examination of that paper's supplementary information indicates that they have produced projections for multiple tide-gauges in Singapore, including the Raffles Light House tide gauge. For 2100 in RCP 4.5 and 8.5, their likely ranges of 35-79 cm and 54-102 cm, respectively, are in general good agreement with the authors' projections (29-73 cm and 45-102 cm), though Kopp et al. (2014) attempts to characterize the tail risk as well (for example, for RCP 8.5, they find a 95th percentile projection of 127 cm, and 99.5th percentile projection of 193 cm, and a maximum physically plausible projection of 275 cm). Kopp et al. (2014)'s SI also provides a process-level breakdown for each tide gauge similar to the authors' Table 2.

The likely ranges from Kopp et al (2014) for several Tide Gauge sites (shown below) have been compared to our results. We note that the authors also include a “Background rate”, which originates from a Gaussian process model applied to the tide gauge records, and includes GIA, tectonics and other non-climatic local effects as a linear trend. We also note that the numbers in Kopp are computed relative to the year 2000, whereas the numbers in this paper are computed relative to the mean for 1986-2005.

Tide Gauge	RCP4.5 change @ 2100 (cm)		RCP8.5 change @ 2100 (cm)	
	No GIA/Bkgd	With GIA/Bkgd	No GIA/Bkgd	With GIA/Bkgd
Raffles Light -0.97 mm/yr	55 [35-79]	45 [25-69]	76 [54-102]	66 [41-89]
Tanjong Pagar -0.29 mm/yr	62 [40-88]	59 [37-85]	83 [59-111]	80 [56-108]
Tuas -0.4 mm/yr	62 [30-96]	58 [26-92]	83 [49-119]	79 [45-114]
<b>Mean of 3 gauge sites</b>		<b>54 [29-82]</b>		<b>75 [47-103]</b>
<b>SV2 Values</b>		<b>52 [29-73]</b>		<b>74 [45-102]</b>

Based a comparison of our data to the above results the following comment has been incorporated into the text:

“Our estimates of time-mean sea level change for Singapore are in good agreement with sea level projections at tide-gauge sites in Singapore produced by Kopp et al (2014). Those authors report a likely range of 29-82 cm (47-103 cm) over the 21<sup>st</sup> Century under RCP4.5 (RCP8.5) based on the average of three tide gauge sites, after local GIA and other non-climatic effects have been taken into account.”

35 Page 2958, line 16: The authors may find useful information for their intro on pre-observational  
36 Holocene sea-level change in Singapore from Bird MI, Austin WEN, Wurster CM, et al. Punctuated  
37 eustatic sea-level rise in the early mid-Holocene. *Geology*. 2010;38:803–6. doi:10.1130/G31066.1.

38 The following text has been added to the introduction:

39 “Bird et al. (2010) consider the impact of pre-observational (early Holocene) sea level change on  
40 human dispersal in coastal regions of Singapore, and provide evidence of the rapid rate at which  
41 regional sea levels changed during this period. The authors suggest sea levels rose at a rate of 1.8 m  
42 100 yr<sup>-1</sup> between 8900 and 8100 calibrated yr B.P., exhibited little change in between 7800 and 7400  
43 calibrated yr B.P. and then a rose by 4–5 m by 6500 calibrated yr B.P.”

44

45 Page 2958, line 20: As the authors correctly note later, the dominant GIA process in Singapore is  
46 continental levering. “Glacial isostatic rebound” generally refers to the uplift of the solid Earth that  
47 happens at the former location of ice sheets.

48 Where used “isostatic rebound” has been replaced throughout the text with “isostatic adjustment”

49

50 Page 2959, line 7: RCP 4.5 can be a “mid-range estimate of expected change” only if you place a  
51 probability distribution on policy choices. It is almost impossible to obtain without deliberate climate  
52 policy and so is not comparable to SRES B2. (Note that, in the comparison study of Rogelj et al.,  
53 2012 (doi:10.1038/NCLIMATE1385), SRES B2 had a likely warming 2.6–3.7 C in 2100, while RCP 4.5  
54 had a likely warming of 2.0–3.0C.

55 We replace “mid-range estimate” with the phrase used by Kopp et al (2014) “moderate mitigation  
56 policy scenario”

57

58 Page 2960, line 2: Work subsequent to AR5 has attempted to fill in the sea-level rise probability  
59 distribution beyond the likely range (e.g., Kopp et al., 2014, doi:10.1002/2014EF000239, and  
60 Jevrejeva et al., 2014, doi:10.1088/1748-9326/9/10/104008), so I do not think it is accurate to say that  
61 the IPCC “likely range represents the best scientific assessment of global sea level change available  
62 at present.”

63 The existing text:

64 “The upper and lower limits of each time series represent the “likely range” of GMSL change, taking  
65 the IPCC AR5 assessment that there is a > 66 % chance that the observed sea level rise would fall  
66 within these bounds for a given RCP. The additional uncertainty implied by this arises from the  
67 authors’ expert judgement of methodological or structural uncertainty that is not captured by the  
68 CMIP5 ensemble, and the likely range represents the best scientific assessment of global sea level  
69 change available at present.”

70 has been replaced with:

71 “The upper and lower limits of each time series represent the “likely range” of GMSL change, taking  
72 the IPCC AR5 assessment that there is a >= 66 % chance that the observed sea level rise would fall  
73 within these bounds for a given RCP. The additional uncertainty implied by this arises from the  
74 authors’ expert judgement of methodological or structural uncertainty that is not captured by the  
75 CMIP5 ensemble.”

76 In addition the text in the discussion:

77 "There are several caveats to the sea level, surge and wave projections presented in this study and  
 78 we consider each in turn in the following paragraphs. Mean sea level projections are presented as  
 79 likely (66–100 % probability) ranges for the RCP4.5 and RCP8.5 scenarios of future greenhouse gas  
 80 concentrations, taking into account a number of uncertainties that cannot be formally quantified with  
 81 the present state of scientific knowledge. As noted previously, sea level projections do not account for  
 82 the unlikely event of a collapse of the marine-based sectors of the Antarctic ice sheet."

83 has been replaced with:

84 "There are several caveats to the sea level, surge and wave projections presented in this study and  
 85 we consider each in turn in the following paragraphs. Mean sea level projections are presented as  
 86 likely (66–100 % probability) ranges for the RCP4.5 and RCP8.5 climate change scenarios, taking  
 87 into account a number of uncertainties that cannot be robustly quantified with the present state of  
 88 scientific knowledge. We note that recent studies have attempted to provide information outside of the  
 89 IPCC likely range (Kopp et al., 2014; Jevrejeva et al., 2014) and this is an important topic of ongoing  
 90 discussion by the research community (Hinkel et al., 2015). As noted previously, our sea level  
 91 projections do not account for the unlikely event of a collapse of the marine-based sectors of the  
 92 Antarctic ice sheet."

93 References included in the above paragraph have been added to the reference list.

94

95 Page 2960, line 9: Please spell out what is meant by a 'nearest neighbor' approach. Why was a  
 96 nearest neighbor approach taken in lieu of directly calculating the finger-prints for the geographic  
 97 coordinates of Singapore?

98 The text:

99 "derived from the Slangen et al. (2014) fingerprints, using a "nearest neighbour" approach."

100 has more accurately been replaced with:

101 "derived from the Slangen et al. (2014) fingerprints, using the closest 1 x 1 degree grid box".

102

103 Page 2960, line 13: ICE 5G is an ice model, not a GIA model. To produce a GIA model, an ice model  
 104 must be combined with a model specifying mantle viscosity and lithospheric thickness (e.g., ICE5G  
 105 might be combined with the VM2-90 rheological model, yielding the GIA model ICE5G-VM2-90).  
 106 Please clarify what rheological model was used with the ICE5G ice model.

107 The rheological model used is VM2 L90, usually it is referred to as ICE-5G(VM2) - see  
 108 <http://www.atmosp.physics.utoronto.ca/~peltier/data.php>. This is now stated in the text as follows:

109 "Rates of glacial isostatic adjustment (GIA) for Singapore were determined using the combined ice  
 110 and rheological models ICE-5G(VM2) (Peltier, 2004;  
 111 <http://www.atmosp.physics.utoronto.ca/~peltier/data.php>), provided by Slangen et al. (2014),"

112

113 Page 2960, line 22: Other authors (e.g., Kopp et al., 2014) use the term "oceanographic" rather than  
 114 "steric/dynamic" (or "steric+dynamic", as it appears in Slangen et al. 2014). Neither term appears to  
 115 be used in Church et al. (2013).

116 We have replaced "steric/dynamic" with "oceanographic" throughout.

117

118 Page 2960, line 26: What is the resolution of the GCM being examined to estimate the dynamic sea  
 119 level terms? Are there any studies using high-resolution regional models to estimate sea-surface  
 120 height, with which the GCMs might be compared?

121 We are not aware of any regional studies using high resolution ocean models with which to compare  
 122 the GCMs.

123 The text:

124 "However, all models show relatively weak gradients in the pattern of change in the vicinity of  
 125 Singapore, a result that appears to be largely independent of the underlying model resolution."

126 Has now been replaced with:

127 "However, all models show relatively weak gradients in the pattern of change in the vicinity of  
 128 Singapore. This result appears to be largely independent of the underlying ocean model resolution,  
 129 which varies across the CMIP5 models from about 2° to 0.3°"

130

131 Page 2961, line 6-9: The authors linear scaling of dynamic sea-level with thermal expansion seems a  
 132 weak, or at least poorly explained, point in their analysis. What is the evidence that all models show a  
 133 linear relationship between local steric/dynamic sea-level change and global thermal expansion? The  
 134 authors should show this evidence. But if the authors have the evidence to show this (which they  
 135 should), why don't they just use the CMIP5 projections of steric/dynamic change directly?

136 A new figure has been added to the supplementary material (Figure A1) showing the relationship  
 137 between local steric/dynamic sea-level change and global thermal expansion for each CMIP5 model.  
 138 This figure is also included at the end of this document for reference.

139 Effectively, we are using the steric+dynamic (now referred to as "oceanographic") change directly. We  
 140 follow the IPCC AR5 method of computing the difference in sea level based on two 20-year periods to  
 141 characterise the change signal and uncertainty at the end of the 21<sup>st</sup> Century. However, we also want  
 142 a method to describe how this signal emerges over time. Since the regional oceanographic sea level  
 143 change scales nicely with global mean sea level for all models we use the ensemble mean thermal  
 144 expansion as a basis for a smoothly evolving time-series for both oceanographic sea level change  
 145 and its associated uncertainty.

146

147 Page 2962, line 12: "IPPC" is misspelled.

148 This has been corrected

149

150 Figure 2: While the difference between SMB and dynamic fingerprints for Antarctica makes sense (I  
 151 assume it is due to SMB being dominated by East Antarctica and dynamic by West Antarctica), the  
 152 reason they are different for Greenland is less obvious. Please explain.

153 SMB on both ice sheets is prescribed as a uniform distribution over the entire ice sheet. The  
 154 dynamics are specified to regions: for Antarctica it's the Antarctic Peninsula, Amundsen Sea

155 embayment and a small amount in East Antarctica. For Greenland, the dynamical contribution is  
156 situated on the southern tip and along the west coast of the ice sheet.

157

158 Table 4: Values in the text are quoted in mm/century, which are more useful units.

159 Table 4 has been converted to mm/century

160

161 Table 5: There is a mismatch between the units specified in the caption (m/century)

162 and the values quoted in the text (mm/century). I presume the latter is correct.

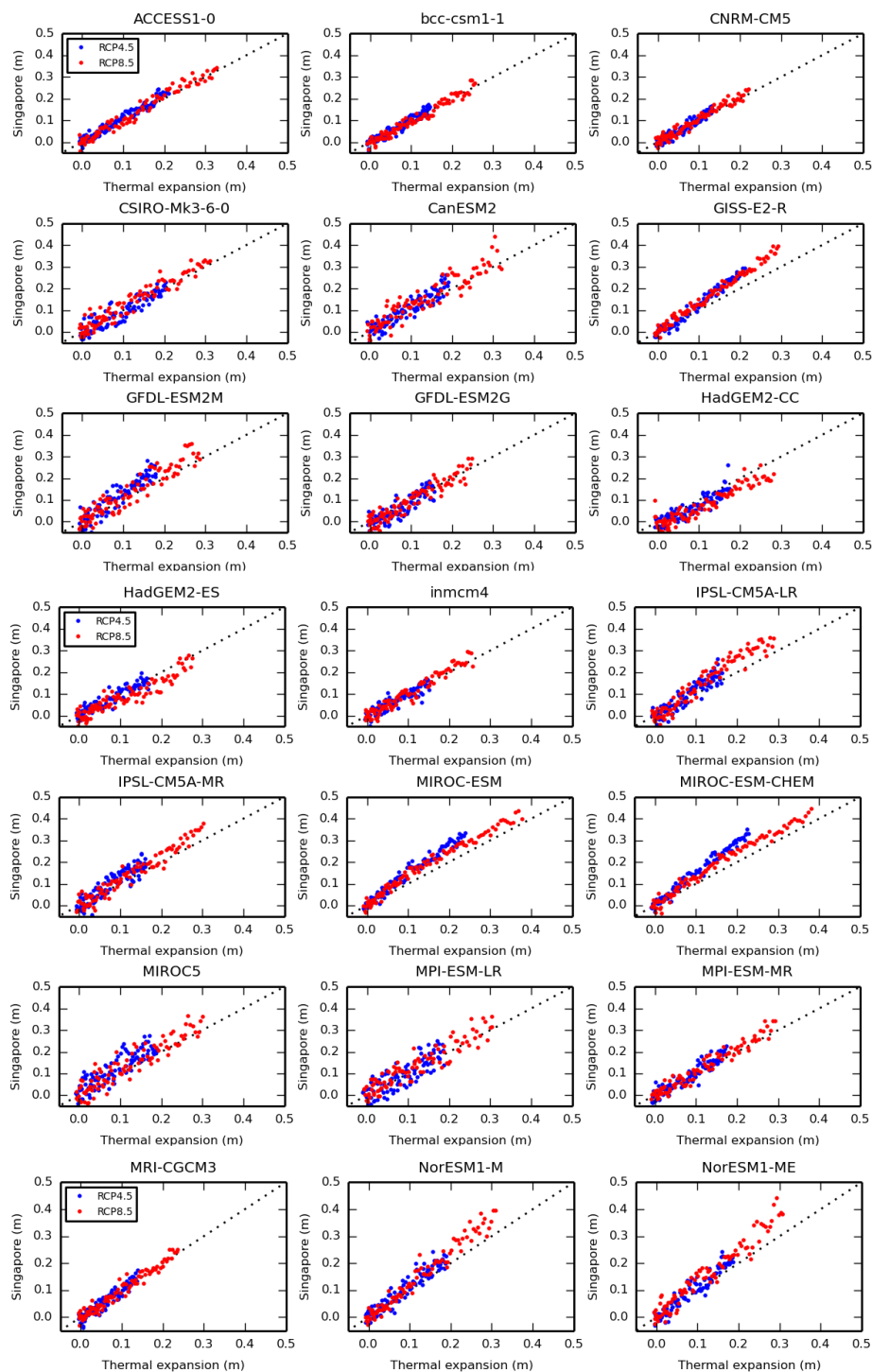
163 Table 5 has been converted to mm/century

164

165

166

167



169 **Response to comments from reviewer #2**

170 Specific comments:

171 p. 2958, line 14: "during the northwest monsoon" - you meant the northeast monsoon, per p. 2957,  
172 line 27?

173 Yes, this has been corrected

174 p. 2961, lines 21-22: when is the central estimate based on the median, and when isn't it?

175 For all of the time series presented in the IPCC AR5 supplementary materials the central estimate is  
176 the median value (50th percentile). However, when we computed the local steric+dynamic(now  
177 oceanographic) terms we did this by computing the ensemble mean. So the oceanographic term is  
178 based on a mean and in all other cases the median is used. This is now clarified in the text as  
179 follows:

180 "Time series of each of the terms listed in Table 1 have a central estimate (based on the median for  
181 all terms except the oceanographic term, for which the mean is used)"

182

183 p. 2962, lines 4-5: specifically Greenland and Antarctic ice dynamics, which should be stated at least  
184 here once for clarity

185 This is stated in the preceding sentence.

186 p. 2964, lines 1-2: Is there any way that you can add to this sentence so that it is a bit more  
187 accessible (i.e., so that the data consequences of this choice are more clear) to those who are not  
188 familiar with this particular regional model?

189 The sentence:

190 "it was necessary to modify the z-envelope (which allows sigma levels to intercept land in regions of  
191 steep topography) such that the minimum number of layers in the vertical was set to 7"

192 Has been replaced with:

193 "it was necessary to modify the z-envelope (which allows sigma levels to intercept land in regions of  
194 steep topography, thus preventing steep gradients in the vertical levels that may introduce pressure  
195 gradient errors) such that the minimum number of vertical levels at any location was 7"

196

197 p. 2968, lines 7-8: Was any testing done to see if changes to the shape within a given simulation's  
198 GEV distribution were small?

199 We did not investigate changes in the shape parameter in this work, however our experiments with  
200 climate-model-forced century-scale storm surge simulations for the UK have suggested little or no  
201 added value in allowing the shape parameter to change. The approach of allowing change in the  
202 location and scale parameters (but not the shape parameter) has some precedent, for example:

203 Butler, A., Heffernan, J.E., Tawn, J.A., Flather, R.A. and Horsburgh, K.J. (2007) Extreme value  
204 analysis of decadal variations in storm surge elevations. Journal of Marine Systems 67 pp189-200

205 Howard, Lowe and Horsburgh (2010). Interpreting century-scale changes in southern North Sea  
 206 storm surge climate derived from coupled model simulations. Journal of Climate. Volume 23, Issue 23  
 207 (December 2010) pp 6234-6247

208 Zhang, X, Zwiers, F and Li, G, 2004. Monte Carlo Experiments on the Detection of Trends in Extreme  
 209 Values. Journal of Climate. 17, 1945-1952

210 Zang et al (2004) state that:

211 "Trend in the shape parameter  $\xi$  is not considered in this study because we decided to avoid the  
 212 complications that arise from allowing all three GEV parameters to vary in time. We assume that it is  
 213 not likely for there to be significant change in the shape of the tails of the kinds of variables that are  
 214 typically considered in climate studies over the period of record (less than 100 yr) that is ordinarily  
 215 available for analysis. Situations in which the tail does lengthen, or shorten, modestly relative to the  
 216 main body of the distribution can be dealt with approximately by varying the scale parameter."

217

218 p. 2969, lines 25-26: Does this not also suggest that the interannual variability for extreme water  
 219 levels has not changed very much over the projected 130 years? This should also be explicitly  
 220 mentioned.

221 Yes, this is now clearly stated.

222

223 p. 2974, lines 7-11: This is the estimation for a possible upper limit on the changes in local sea level  
 224 which I mentioned in the general comments. It is a citation from another source, but I wonder if it  
 225 might be good to include a high estimate of possible (maybe at the 90% level) sea level change plus  
 226 storm or wave events, in order to put a number on what could be expected by 2100 in order to plan  
 227 protection measures and infrastructure. Making such an estimate is not something which I believe you  
 228 must do for the paper to be publishable; it's merely a suggestion.

229 We do not include this information in the current paper, however, we suggest in the text that "site  
 230 specific projections of future extreme still water level can be obtained by linearly combining return  
 231 levels derived from tide gauge data with the sea level change projections presented in Table 3. (Tide-  
 232 gauge data represent the best information available about present-day location-specific return levels,  
 233 however, it is worth noting that uncertainties in the present-day return levels derived from relatively  
 234 short tide-gauge records are likely to be a large component of the combined uncertainty in projected  
 235 future return-level curves.) In the longer term there is potential to develop better estimates of current  
 236 risk by combining model-derived information with observed time series. The skew surge joint  
 237 probability method (Batstone et al., 2013) provides an approach to addressing this problem."

238

239 - - - - Reference errors:

240 All reference errors have been corrected.

241 p. 2957, lines 9-10: Christensen et al., 2013 should be Church et al. 2013 line 11: Allen et al. 2010  
 242 and Penduff et al. 2010 are not in the References line 24: Maren, 2012 not in the References

243 p. 2963, line 19: Madec, 2008 not in the References

244 p. 2967, line 16: Huerta and Bruno, 2007 (not just Huerta) lines 16-17: Kotz and Nadarajah, 2000 line  
 245 17: Méndez et al., 2007,2008



246

247 ----- Some correction suggestions:

248 All of the following corrections have been applied as suggested.

249 p. 2964, line 4: "For the case of the 4 GCM-forced simulations," (add a comma) lines 24-25: "In order  
250 to allow calculation of skew surge, an..." (add a comma after 'surge')

251 p. 2965, line 25: "Three-hourly wind data were..." (not 'was')

252 p. 2969, line 7: This is the next new figure referenced after Fig. 3 on p. 2960. The next numbered Fig.  
253 should be Fig. 4 (which is referenced in the following major section). Renumber and reorder the  
254 figures; this way you won't get yelled at later by the editing department.

255 p. 2969, line 17: 18-yr (or 18-year) line 18: I would reword "like-for-like" as "fair". Also, insert a comma  
256 after "comparison". line 20: 130-yr

257 p. 2970, line 18: "state of the art" I'm not fond of quotes or the use of the term 'socalled' when  
258 qualifying something. It can sound like you don't believe it is true, or that C1469 OSD 12, C1467–  
259 C1470, 2016 Interactive Comment Full Screen / Esc Printer-friendly Version Interactive Discussion  
260 Discussion Paper you are quoting an unnamed person. Also, this adjective is itself sometimes  
261 criticized. I would suggest removing the entire thing, as it isn't really needed to make the point.

262 p. 2971, line 25: comma after 'timescale' and 'pathway'

263 p. 2972, line 17: comma after '77%' line 28: comma after 'simulations' p. 2975, line 26: change  
264 comma after 'activity' to a semicolon

265 |

266 |

267 |

268

269

270

271

272

273

274

275

276

277

278

279

280

281

Manuscript including track changes:

## Projected sea level rise and changes in extreme storm surge and wave events during the 21<sup>st</sup> century in the region of Singapore

Heather Cannaby<sup>1</sup>, Matthew D. Palmer<sup>2</sup>, Tom Howard<sup>2</sup>, Lucy Bricheno<sup>1</sup>, Daley Calvert<sup>2</sup>, Justin Krijnen<sup>2</sup>, Richard Wood<sup>2</sup>, Jonathan Tinker<sup>2</sup>, Chris Bunney<sup>2</sup>, James Harle<sup>1</sup>, Andrew Saulter<sup>2</sup>, Clare O'Neill<sup>2</sup>, Clare Bellingham<sup>1</sup>, Jason Lowe<sup>2</sup>

<sup>1</sup>National Oceanography Centre, 6 Brownlow Street, Liverpool, L3 5DA, UK

<sup>2</sup>Met Office, Fitz Roy Road, Exeter, Devon, EX1 3PB, UK

Corresponding author contact details: e-mail: [heanna@noc.ac.uk](mailto:heanna@noc.ac.uk), Tel: +44 151 795 4848, Fax: +44 (0)151 7954801

### Abstract

Singapore is an island state with considerable population, industries, commerce and transport located in coastal areas at elevations less than 2 m making it vulnerable to sea-level rise. Mitigation against future inundation events requires a quantitative assessment of risk. To address this need, regional projections of changes in (i) long-term mean sea level and (ii) the frequency of extreme storm surge and wave events have been combined to explore potential changes to coastal flood risk over the 21<sup>st</sup> century. Local changes in time mean sea level were evaluated using the process-based climate model data and methods presented in the IPCC AR5. Regional surge and wave solutions extending from 1980 to 2100 were generated using ~12 km resolution surge (Nucleus for European Modelling of the Ocean - NEMO) and wave (WaveWatchIII) models. Ocean simulations were forced by output from a selection of four downscaled (~12 km resolution) atmospheric models, forced at the lateral boundaries by global climate model simulations generated for the IPCC AR5. Long-term trends in skew surge and significant wave height were then assessed using a generalised extreme value model, fit to the largest modelled events each year. An additional atmospheric solution downscaled from the ERA-Interim global reanalysis was used to force historical ocean model simulations extending from 1980-2010, enabling a quantitative assessment of model skill. Simulated historical sea surface height and significant wave height time series were compared to tide gauge data and satellite altimetry data respectively. Central estimates of the long-term mean sea level rise at Singapore by 2100 were projected to be 0.52 m(0.74 m) under the RCP 4.5(8.5) scenarios respectively. Trends in surge and significant wave height 2-year return levels were found to be statistically insignificant and/or physically very small under the more severe RCP8.5 scenario. We conclude that changes to long-term mean sea level constitute the dominant signal of change to the projected inundation risk for Singapore during the 21<sup>st</sup> century. We note that the largest recorded surge residual in the Singapore Strait of ~84 cm lies between the central and upper estimates of sea level rise by 2100, highlighting the vulnerability of the region.

**Keywords:** Singapore, SE Asia, Sea level rise, Climate change, Significant wave height, Storm surge

## 1. Introduction

Singapore is an island state with considerable population, industries, commerce and transport located in coastal areas at elevations less than 2 m (Wong, 1992). Singapore is thus potentially exposed to the effects of sea level rise and climate induced changes in extreme events. Mitigation against future inundation events requires a quantitative assessment of risk. Global scale climate projections generated for the Intergovernmental Panel on Climate Change Assessment Reports (Meehl et al., 2007; Church et al., 2013) are generally on too coarse a grid scale to provide relevant information at the regional scale (e.g. Allen et al., 2010; Penduff et al., 2010). Hence the assessment of climate change impacts on regional coastlines requires a focused regional study. To address this need regional projections of changes in (i) long-term mean sea level and (ii) the frequency of extreme storm surge and wave events have been combined to explore potential changes to coastal flood risk in Singapore over the 21<sup>st</sup> century. The following paragraphs briefly summarise the processes which influence temporal variability in sea level in the Singapore Strait.

Located in the middle of the Sunda shelf, the Singapore Strait (Figure 1a) is connected via the South China Sea to the Pacific Ocean in the northeast, to the Java Sea in the southeast, and via the Malacca Strait to the Indian Ocean in the west. Regional tides are complex with several amphidromic points located in the South China Sea. Tides propagate into the Singapore Strait via the Malacca Strait and from the open seas to the east, resulting in a complex mix of diurnal and semi-diurnal tides observed around the coastline of Singapore (Marengere and Gerritsen, 2012). The mean tidal range at Singapore is ~2 m and the spring maximum range is ~3 m.

The weather in Singapore is influenced by the northern and southern hemisphere monsoon systems. Winds are from the north and northeast during the northeast monsoon season, which extends from December to early March and from the south or southeast during the southwest monsoon season which extends from June to September. In response to the monsoon winds, sea level in the Singapore Strait exhibits seasonal variability of the order  $\pm 20$  cm, being highest during the northeast monsoon when the fetch is greatest. Extreme sea level anomaly events in Singapore tend to coincide with prolonged (lasting for several days in duration) northeast winds over the South China Sea during this season (e.g. Tkalich et al., 2009). Interannual variability in sea level is dominated by El Nino and La Nina events which cause the Sea Surface Height (SSH) to vary by  $\pm 5$  cm, with lower SSH observed during El Nino events (Tkalich et al. 2013).

The sheltered location of Singapore results in significant wave heights that are typically less than 1 m. Waves of close to 1 m in height occur along the southwest coast during squall events associated with the southwest monsoon. However, extreme wave events occurring during the northwest monsoon have the potential to be more damaging due to the higher sea level during this season.

Tkalich et al. (2013) report that sea level in the Singapore strait has been rising at an average rate of 1.2-1.7 mm yr<sup>-1</sup> between 1975 and 2009, 1.8-2.3 mm yr<sup>-1</sup> between 1984 and 2009 and 1.9-4.5 mm yr<sup>-1</sup> between 1996 and 2009. The trend is larger than the global mean during the earlier period and smaller during the latter period. Over multi-decadal timescales, accounting for glacial isostatic adjustment rebound, sea level in the Singapore Strait has been rising at approximately the same rate as the global mean. Bird et al. (2010) consider the impact of pre-observational (early Holocene) sea level change on human dispersal in coastal regions of Singapore, and provide evidence of the rapid rate at which regional sea levels changed during this period. The authors suggest sea levels rose at a rate of 1.8 m 100 yr<sup>-1</sup> between 8900 and 8100 calibrated yr B.P., exhibited little change in between 7800 and 7400 calibrated yr B.P. and then a rose by 4–5 m by 6500 calibrated yr B.P.

## 2. Methods

Change in the long-term climate of extreme sea level can arise due to (i) change in regional time-mean relative sea level and (ii) change in the frequency/intensity of extreme events. There is evidence from dynamical modelling studies based in the North Sea (e.g. Howard et al., 2010; Sterl et al., 2009) and the Gulf of Mexico (e.g. Smith et al., 2010) that these two components of change can be modelled separately and then combined linearly to give a total projected extreme sea level change. This is the approach taken in this study, although we note that this finding is not necessarily applicable to all locations (e.g. Mousavi et al., 2011; Smith 2010).

In this study climate projections are generated for two Representative Concentration Pathways (RCPs, Meinshausen et al., 2011), these being RCP4.5 and RCP8.5. The IPCC describe RCP4.5 as an intermediate emissions scenario and it was chosen to provide a moderate mitigation policy scenario ~~mid-range estimate of expected change~~. RCP4.5 is comparable to the SRES scenario B1, used in the IPCC AR4 and is consistent with a future with relatively ambitious emissions reductions. RCP8.5 is described as a high emissions scenario and is consistent with a future with no policy changes to reduce emissions. RCP8.5 was chosen to provide an upper estimate of expected change (Meinshausen et al., 2011).

### 2.1 Calculation of local changes in time-mean sea level

Projections of global mean sea level (GMSL) rise have been presented by the IPCC AR5 (Church et al., 2013) for a range of climate change scenarios. These projections include estimates of: (1) global thermal expansion, (2) ice sheet mass changes from surface mass balance, (3) ice sheet mass changes from ice dynamics, (4) glacier mass changes and (5) changes in land water (from ground water extraction and reservoir impoundment). Time series for each component (1)-(5), under different RCPs, over the 21<sup>st</sup> Century are available from the IPCC AR5 Chapter 13 supplementary data files (<http://www.climatechange2013.org/report/full-report/>). These time series are derived from the direct output of climate models (1), combining climate model projections with empirical relationships and/or glacier models (2 and 4) and bounding scenarios based on the scientific literature (3 and 5). ~~The upper and lower limits of each time series represent the "likely range" of GMSL change, taking the IPCC AR5 assessment that there is a > 66% chance that the observed sea level rise would fall within these bounds for a given RCP. The additional uncertainty implied by this arises from the authors' expert judgement of methodological or structural uncertainty that is not captured by the CMIP5 ensemble, and the likely range represents the best scientific assessment of global sea level change available at present.~~ The upper and lower limits of each time series represent the "likely range" of GMSL change, taking the IPCC AR5 assessment that there is a >= 66 % chance that the observed sea level rise would fall within these bounds for a given RCP. The additional uncertainty implied by this arises from the authors' expert judgement of methodological or structural uncertainty that is not captured by the CMIP5 ensemble.

Local changes in time mean sea level associated with ocean mass changes (2-5 above) over the 21<sup>st</sup> Century are evaluated using the fingerprint patterns of Slangen et al. (2014), which represent the ratio of a local sea level change to a unit rise in GMSL for each contributing term. Time series of each term obtained from the AR5 supplementary data files (available at <http://www.climatechange2013.org/report/full-report/>) were converted into local values for Singapore by multiplying by a local scaling factor (Table 1) derived from the Slangen et al. (2014) fingerprints, using the closest 1 x 1 degree grid box ~~derived from the Slangen et al (2014) fingerprints, using a~~

~~"nearest neighbour" approach.~~ Maps showing the ratio of local relative sea level change per unit of GMSL rise due to Greenland and Antarctica surface mass balance terms and changes in glacial ice content and land water use are shown in Figure 2. Rates of glacial isostatic adjustment (GIA) for Singapore were determined using the ~~combined ice and rheological models ICE-5G(VM2) ICE5G~~ (Peltier, 2004; <http://www.atmosp.physics.utoronto.ca/~peltier/data.php>) ~~estimates~~, provided by Slangen et al. (2014), again ~~taking data from the closest 1 x 1 degree grid box assuming a "nearest neighbour" approach~~ (Figure 2f). Given the long timescales associated with GIA, the rates of change are assumed to be constant and independent of climate change scenario.

Local changes in ocean density (steric change) and circulation are also important for projections of regional sea level (e.g. Pardaens et al., 2011). We follow the approach taken in IPCC AR5 (Church et al., 2013; Slangen et al., 2014) and combine changes in local dynamic sea level (which represents local departures from global mean sea level) with changes in global thermal expansion to estimate the combined effects of local density and ocean circulation (the ~~"oceanographicsteric/dynamic"~~ term). As has been shown by previous studies (Pardaens et al., 2011, Slangen et al., 2014), we find a large model spread in projections of regional ~~oceanographicsteric/dynamic~~ sea level rise (Figure 3). ~~However, all models show relatively weak gradients in the pattern of change in the vicinity of Singapore, a result that appears to be largely independent of the underlying model resolution. However, all models show relatively weak gradients in the pattern of change in the vicinity of Singapore. This result appears to be largely independent of the underlying ocean model resolution, which varies across the CMIP5 models from about 2° to 0.3°~~

The sensitivity of results to the choice of grid box was tested by selecting a primary and secondary grid box to represent Singapore. The difference in multi-model median estimates between boxes is about  $\pm 1$  mm and  $\pm 2$  mm for RCP4.5 and RCP8.5 respectively. This represents less than 1% of the change signal and therefore is considered a negligible uncertainty. In order to provide an estimate of the projected ~~oceanographicsteric/dynamic~~ sea level rise that is continuous with time, it was assumed that the change signal (and model spread) emerges proportionally to the global thermal expansion time series of the IPCC AR5. This approach is justified since, to a good approximation, all models show a linear relationship between the local ~~oceanographicsteric/dynamic~~ sea level change near Singapore, and global thermal expansion ~~(this relationship is demonstrated in Figure A1 for all CMIP5 models for RCP4.5 and RCP8.5)~~. This permits us to estimate the sea level change for the Singapore region throughout the 21st century for each scenario.

IPCC AR5 estimates of the effect of changes in atmospheric loading for the RCP4.5 and RCP8.5 scenarios are available as part of the Chapter 13 supplementary data files (Church et al., 2013). However, the projections for the Singapore region are very small compared to the other terms – representing only about 1% of the total estimated sea level change, with relatively little spread among different model projections. Given the substantial combined uncertainties of the leading terms in total sea level change, we do not include the inverse barometer effect in our final projections as we consider this term constitutes a negligible contribution to projected sea level change.

The sea level change for Singapore was computed as the difference between the 1986-2005 and 2081-2100 periods. The median of the model ensemble change was taken as the central estimate and the 5th and 95th percentiles were calculated based on the multi-model standard deviation, assuming a normal distribution. Time series of each of the terms listed in Table 1 have a central estimate ~~(often based on the median for all terms except the oceanographic term, for which the mean is used)~~ and both an upper and lower bound, which are indicative of the 5th and 95th percentiles of the distribution and/or the likely range assessed in the IPCC AR5. The central estimates of the different components are simply added together to arrive at values for total sea level change at

Singapore. To combine the associated uncertainties we follow the approach outlined by Church et al (2013), in which total uncertainty ( $\sigma_{\text{tot}}$ ) expressed as a variance is estimated according to Eq (1),

$$\sigma_{\text{tot}}^2 = (\sigma_{\text{oceansteric/dyn}} + \sigma_{\text{smb\_a}} + \sigma_{\text{smb\_g}})^2 + \sigma_{\text{glac}}^2 + \sigma_{\text{LW}}^2 + \sigma_{\text{dyn\_a}}^2 + \sigma_{\text{dyn\_g}}^2 \quad \text{Eq (1)}$$

where  $\sigma_{\text{oceansteric/dyn}}$ ,  $\sigma_{\text{smb\_a}}$ ,  $\sigma_{\text{smb\_g}}$ ,  $\sigma_{\text{glac}}$ ,  $\sigma_{\text{LW}}$ ,  $\sigma_{\text{dyn\_a}}$ , and  $\sigma_{\text{dyn\_g}}$  represent uncertainties in sea level rise projections due to changes in oceanographicsteric/dynamic processes, Antarctic surface mass balance, Greenland surface mass balance, glaciers, land water, Antarctic dynamics and Greenland dynamics respectively. It is assumed that the first three terms—which have a strong correlation with global air temperature have correlated uncertainties and can therefore be added linearly. This combined uncertainty is then added to the other components' uncertainties in quadrature. The uncertainties in the projected ice sheet surface mass balance changes are reported to be dominated by the magnitude of climate change, rather than their methodological uncertainty (see AR5 Chapter 13 supplementary materials for details), while the uncertainty in the projected glacier change was assumed to be dominated by methodological uncertainty. We do not include an uncertainty contribution for GIA or the inverse barometer effect (which as noted above has a negligible contribution to sea level projections at Singapore) in our method.

## 2.2 Design of model study

The surge and wave projections described in this work were conducted utilising high resolution (12 km) regional atmospheric simulations, forced at the open boundaries by a selection of 9 GCM solutions generated for the IPCC AR5 (IPCC AR4, 2007; see McSweeney et al., 2013 and McSweeney et al 2015 for further details on downscaled atmospheric simulations). Figure 1a shows the downscaled atmospheric model domain. Computational expense dictated the need to select only the most suitable GCMs from which to generate downscaled atmospheric solutions. Approaches for selecting climate models for downscaling are discussed in various papers (e.g. Wilby et al., 2009, Whetton et al 2012). Criteria of particular importance in selecting climate models for impact studies include (a) that the climate models under historical conditions accurately represent the processes or features that are of particular relevance to the impact study and (b) that the climate models sample the range of projected change in the features of interest (Whetton et al, 2012). Both these criteria were considered when selecting models for downscaling. In particular, it was essential that the GCMs used should appropriately represent wind speed during both the northern and southern hemisphere monsoon systems. Selection was further constrained by the availability of suitable data on the CMIP5 archive. Of nine downscaled atmospheric simulations conducted, four were selected to force the high resolution surge and wave models: HadGEM2-ES, CNRM-CM5, IPSL-CM5A-MR, and GFDL-CM3. These four models sample a range of projected change in wind speed and include the model GFDL-CM3 which out of the nine downscaled atmospheric simulations exhibited the largest area-averaged change in 850 hPa wind speeds during both the SW and NE monsoon seasons. Computational expense also dictated that downscaled ocean simulations could only be conducted for a single RCP. We therefore chose RCP8.5, which is expected to give the largest climate change signal.

Surge and wave climate projections were generated extending from 1970-2100. An additional atmospheric solution downscaled from the ERAinterim (Dee et al., 2011) global atmospheric reanalysis was used to force historical surge and wave simulations extending from 1980-2010. These historical simulations were used to compare model results with contemporary observations.

## 2.3 Description of surge model

504 The model used to generate surge projections was the Nucleus for European Modelling of the Ocean  
 505 (NEMO) version 3.4 ocean model (www.nemo-ocean.eu, Madec, 2008). NEMO was run with a  
 506 horizontal resolution of 1/12th degree and 9 sigma levels in the vertical. The domain extended from  
 507 95° to 117° East and from 10° South to 17° North as indicated in Figure 1a. Initial conditions specified  
 508 a constant uniform density and this was maintained throughout the simulations by setting surface heat  
 509 and salt fluxes to zero. Hence, NEMO was effectively run as a barotropic model. Tidal forcing was  
 510 applied at the open boundary as a time series of sea-surface elevation representing 15 harmonic tidal  
 511 constituents: Q1, O1, P1, S1, K1, 2N2, MU2, N2, NU2, M2, L2, T2, S2, K2, M4. In order to allow tides  
 512 to propagate through the narrow and very shallow (<12 m in places) Strait of Malacca, it was  
 513 necessary to modify the z-envelope (which allows sigma levels to intercept land in regions of steep  
 514 topography, thus preventing steep gradients in the vertical levels that may introduce pressure gradient  
 515 errors) such that the minimum number of layers in the vertical levels at any location was set to 7. The  
 516 model was run with logarithmic bottom friction and a 4 second barotropic time step. Atmospheric  
 517 forcing was prescribed as hourly mean sea level pressure and 10 m wind fields. For the case of the 4  
 518 GCM-forced simulations, atmospheric forcing was prescribed at the same horizontal resolution as the  
 519 ocean model. ERAinterim (Dee et al, 2011) atmospheric forcing was prescribed at ~80 km resolution.  
 520 Sea surface height was recorded at hourly intervals.

521 The climate models used to generate the atmospheric forcing use different calendar years (only  
 522 CNRM-CM5 uses a Gregorian calendar, GFDL-CM3 and IPSL-CM5A-MR use a 365 day calendar,  
 523 and HadGEM2-ES uses a 360-day calendar. This introduced difficulties in maintaining consistency  
 524 between tidal and atmospheric forcing. Consequently the surge model was not run as a transient  
 525 simulation, rather each year was run independently, following a 5 day spin-up. To avoid splitting  
 526 model simulations during the winter monsoon period when extreme events are most common, the  
 527 model was run 360 days forward in time from 1<sup>st</sup> July. Atmospheric forcing for the 5 day spin-up was  
 528 taken from the last 5 days of June during the start year of the simulation.

529 The surge metric with which we are concerned in this study is skew surge. Skew surge is the  
 530 difference between the elevation of the predicted astronomical high tide and the maximum high water  
 531 observed during the same tidal cycle (e.g. de Vries et al. 1995). Skew surge is considered a more  
 532 significant and practical measure than surge residual (the difference between the predicted  
 533 astronomical tide and the observed water level at any time during a tidal cycle). This is because  
 534 winds are most effective at generating surge in shallow water, meaning peaks in surge residual are  
 535 typically obtained prior to the predicted high water (Horsburgh and Wilson, 2007). In order to allow  
 536 calculation of skew surge, an additional NEMO simulation was conducted extending from 1970 to  
 537 2100 with tidal forcing only (i.e. without any meteorological forcing).

538

## 539 2.4 Description of wave model

540 Wave simulations were performed using WAVEWATCH III (Tolman 1997, 1999a, 2009), a third  
 541 generation wave model developed by NOAA/NCEP. We used version 3.14 with Tolman and Chalikov  
 542 (1996) physics. In a spectral wave model, the choice of source terms dictates how the model  
 543 represents energy input through winds, and dissipation through wave breaking and white capping.  
 544 Regional validation runs were initially performed using two sets of source terms for comparison: WAM  
 545 cycle 4 (Monbaliu 2000) and Tolman and Chalikov (1996). The latter has problems with shorter fetch,  
 546 as wind waves grow slowly and dissipate slowly causing a model bias. WAM cycle 4 has a reduced  
 547 bias overall but also reduced performance in the tropics. Very little difference was found between  
 548 these two source terms for the domain of interest and consequently Tolman and Chalikov (1996)  
 549 source terms were chosen due to the quicker integration time. The regional model was run at 1/12th



degree resolution on a grid extending from 95° East to 117° East and 9° South to 14° North as indicated in Figure 1a. The model was run with a global time step of 900 seconds, a spectral resolution of 30 frequency bins, and 24 directional bins. The model was forced at the surface by hourly mean 10 m wind speed at 1/12th degree resolution. Significant wave height, mean wave energy period, mean wave direction, mean directional spread and mean wave period were recorded at hourly intervals. We focus here on projected changes in significant wave height.

In order to capture swell incoming at the open boundaries of the regional domain, a 50 km resolution global wave model was also run, forced with 3 hourly wind and daily sea ice values taken from the CMIP5 models. The global WW3 domain consisted of a Spherical Multiple Cell grid with a resolution of 0.703125° x 0.4687500°, which extended from ~80°N to 80°S. Three-hourly wind data ~~were~~ not available for the entire future period for IPSL-CM5A-MR, and so daily data were used between 2046 and 2065. The model produced nest files, which were used to force the regional domain at 3 hour intervals.

563

## 564 2.5 Model validation

To assess model performance in simulating local tides, harmonic analyses of modelled and observed sea surface heights were performed using T\_TIDE (Pawlowicz et al., 2002). Comparisons were made at four tide gauge stations situated close to Singapore: Raffles Light House, Kelang, Tanah Merah, and Kukup (see Figure 1b for locations). Simulated SSH time series were extracted from the closest model grid points to the tide gauge locations. Amplitudes and phases of each tidal constituent were then compared using scatter diagrams. During initial test runs the model was tuned by adjusting the bottom friction parameterisation in order to best represent tidal range, and in particular maximum spring high-water events in the immediate vicinity of Singapore.

To assess model performance in representing surge events, simulated annual maximum extreme water levels at grid point 'a' (Figure 1b) were compared to an 18 year (1996-2013) tide-gauge record from Raffles Light House. Six non-overlapping samples of eighteen consecutive years were extracted from each of the model simulations. Return levels were compared to Average Recurrence Interval, (ARI) measured in years. For large return periods ARI is very similar to Return Period (RP; defined as the reciprocal of the annual exceedance probability). ARI and RP are related by Eq (2).

$$579 \quad \text{ARI} = \frac{1}{\log \frac{\text{RP}}{\text{RP}-1}} \quad \text{Eq (2)}$$

The advantage of using ARI is that a Gumbel distribution fitted to the tide gauge observations appears as a straight line on a plot of return level versus ARI, even for small ARI. A Gumbel distribution was fitted to the tide gauge observations and to each of the samples of model data, to give a distribution of model scale parameters. This distribution, along with the scale parameter of the observations, is used to assess whether the observations lie comfortably within the distribution of the model samples.

Modelled significant wave heights were compared to those derived from EnviSat satellite observations (Atlas et al. 2011), utilising the along-track level-2 data collected between 2003 and 2005. Data were obtained via the Globwave data portal (<http://globwave.ifremer.fr/>). All satellite data falling within the model domain during this period were directly compared to the closest model data point in both space and time. A suite of metrics was then generated from the model-data comparisons: mean errors (ME), root mean square errors (RMS), correlation coefficients (PC) and standard deviations (SD).

591



## 2.6 Analysis of extreme events

Analysis of extreme skew surge and significant wave height return levels was limited by the length of the model simulation. Furthermore there was considerable inter-annual variability in both modelled and observed extreme water levels, making long-term trends difficult to identify against the background natural variability. To address these limitations a statistical model was used, firstly to derive return levels for periods longer than the period of the simulation, secondly to better model the behaviour of the system at any given return period, and thirdly to make a more informed assessment of the century-scale trends. The model used was the Generalised Extreme Value (GEV) distribution (e.g. Coles, 2001; Hosking *et al.*, 1985; Huerta [and Bruno](#), 2007; Kotz [and Nadarajah](#)~~*et al.*~~, 2000; Méndez *et al.*, 2007; 2008) applied to annual maximum skew surge and significant wave height values. We tested the impact of using the R largest events (R ranging from 1 to 5) each year, subject to a separation of at least 120 hours in an effort to ensure independence. Results were not strongly sensitive to the value of R, and furthermore for the GFDL and IPSL simulations the parameter estimates did not remain stable as R increased, which is a requirement for making meaningful use of  $R > 1$  (Coles, 2001). Thus for consistency  $R=1$  (annual maxima only) was selected for all simulations. Invoking the External Types Theorem (ETT) we assume that the data are well-approximated by a GEV distribution since each data point is representative of the extreme of a large data block. On fitting a generalised extreme value distribution to the data, the three parameters of the GEV distribution (location, scale and shape) can be used to make statements about the probability of the annual maximum exceeding a particular level. The location parameter of the GEV is analogous to the mean of the normal distribution meaning that a change slides the whole distribution up or down. The scale parameter of the GEV is analogous to the standard deviation of the normal distribution, meaning that an increase widens the spread of the distribution, in the case of the GEV moving the long-period return levels further from the short-period return levels. Thus, a change in either parameter can affect the long-period return levels. In this work we considered the century-scale change in location and scale. It is assumed that the shape parameter remains constant for a given simulation. The GEV distribution was fitted to modelled extreme skew surge and wave heights time series over the 1970-2099 period. Allowing the location parameter to change accommodates potential change in all extreme events (for example at both long and short return periods). Allowing the scale parameter to change accommodates the potential for an increase (or decrease) in the spread of extreme events (for example an increase in intensity of the most extreme surges accompanied by a decrease in intensity of the more frequent surges). A comparison of the quality of the stationary and non-stationary fits gives an indication of the significance of any trend. Linear century-scale trends in return level associated with any given return period were diagnosed from the non-stationary GEV fit to the data. In order to produce a four-model mean ( $\mu$ ) trend estimate, the mean of the ensemble central estimates of trend was taken. The (Bessel-corrected) standard deviation of these four ( $\sigma$ ) then represents the uncertainty in the projection. We then identify ( $\mu - 1.64 \sigma$ ) as the lower bound and ( $\mu + 1.64 \sigma$ ) as the upper bound. Note that the implied symmetry is in the distribution of trends, not the distribution of the extremes themselves, which will in general be asymmetrical. We note that a limitation of the statistical-modelling is an implicit assumption that the behaviour of the extremes in one year is independent of the behaviour of the extremes in neighbouring years. In fact we expect some autocorrelation due to multi-annual cycles in the climate system. This can reduce the effective number of degrees of freedom compared to the number implied by the assumption of independence. In this circumstance there is a risk of diagnosing a trend as statistically significant simply because the assumed number of degrees of freedom is too large. However, we find *a posteriori* that this is not a big issue in this work since we do not diagnose large significant positive trends.

### 3. Model validation

#### 3.1 Surge Model

Comparisons of modelled and observed tidal amplitudes and phases at 4 tide gauge stations (Raffles Light House, Kukup, Tanah Merah, and Keling, located as indicated in Figure 1b) are presented in Figure 4a for the 7 largest tidal constituents (M2, N2, K2, K1, O1, M4 and P1). Modelled tidal amplitudes compare well to those observed, particularly for the dominant semi-diurnal constituents (M2, N2 and K2) for which differences between observed and modelled amplitudes averaged 1.1 cm. The smaller diurnal components (K1, O1, M4, P1) are less well captured by the model with a mean difference between observed and modelled amplitudes of 3 cm. Tidal phase is also well captured by the model (Figure 5b). Modelled and observed tidal phases differed by less than 50°, with the exception at two stations of the smallest amplitude (M4) constituent.

Model skill in simulating extreme events is demonstrated by comparing simulated annual maximum extreme water levels at grid point 'a' with annual maximum events extracted from an 18 year (1996-2013) tide-gauge record at Raffles Light House. In order to make a like-for-like comparison, six non-overlapping samples of eighteen consecutive years were extracted from each of the model simulations. This treatment of the 130-year-long simulations as essentially stationary is justifiable in view of the very small trends described in section 4.2. Extreme still-water return levels from each time series are plotted as a function of return period in Figure 56a. Simulated return levels are approximately 20 cm larger than those derived from observations for all return periods. Importantly, it is also evident that the scale parameter (the gradient in Figure 56a) of the model data is comparable to that of the observations. This reveals that the model is doing a good job of simulating the inter-annual variability (or 'spread') in extreme water levels. The Gumbel distribution, fitted to the observations, is shown by the straight line in Figure 6a. The distribution of model scale parameters derived from the Gumbel distribution fitted to each of the samples of model data and the observations, is shown in Figure 56b. (NB. detrending observed and model data had little effect on the results shown in this plot) It can be seen that the scale parameter of the observations lies comfortably within the distribution of the model samples, indicating that the observed scale parameter is well-modelled and that interannual variability in extreme water levels changes little over the course of the simulations. Aside from the mean sea-level uncertainty, it is the uncertainty in the scale parameter that primarily determines the uncertainty in long-period return levels (i.e. the uncertainty in the most extreme events) under the Gumbel distribution. The good agreement between the modelled and observed scale parameter increases our confidence in applying the model to project century-scale changes in extreme water levels.

#### 3.2 Wave Model

The relationship between simulated significant wave heights and those observed by satellite altimetry across the model domain between 2003 and 2005 is summarised by a correlation coefficient of 0.85, a standard deviation of 0.52 m, and a mean bias of -0.11 m. These statistics demonstrate good model performance, comparable to the UK Met Office's ~~'state-of-the-art'~~ operational wave model performance in tropical regions (Bidlot et al., 2000, Bidlot & Holt, 2006, Bidlot et al., 2007). Qualitative comparison of modelled and observed seasonal mean cycles in significant wave height at Singapore (not shown), demonstrates that the model is able to represent seasonality in significant wave heights at Singapore. A seasonal climatology generated from the ERA-interim forced simulation exhibits maximum significant wave heights of ~0.3 m during the southwest monsoon season and maximum significant wave heights of ~0.35 m during the north ~~eastwest~~ monsoon season. Significant wave heights decrease to ~0.1 m outside of the monsoon seasons.

688

## 689 4. Projections of regional sea level change

### 690 4.1 Time-mean sea level

691 Time series of projected total sea level rise at Singapore and its components for RCP4.5 and RCP8.5  
692 are presented in Figure 6. The changes between 1986-2005 and 2081-2100 for each contributing  
693 component are presented in Table 2. Central, lower and upper ranges of total sea level rise at  
694 Singapore out to 2050 and 2100 are presented in Table 3, alongside global mean values for  
695 comparison. The central estimates of total sea level rise at Singapore are similar to the global mean  
696 projections reported in the IPCC AR5. Glacier and ice sheet surface mass balance terms result in a  
697 larger increase in sea level at Singapore compared to the global mean. This is because there is a far-  
698 field rise in sea level as a result of the associated change in Earth's gravity field as the mass is re-  
699 distributed away from high latitudes (Tamisiea and Mitrovica, 2011). The larger ice mass balance  
700 term is, however, offset by a negative contribution to sea level rise at Singapore from glacial isostatic  
701 adjustment. This is the result of additional ocean mass from the last deglaciation depressing the sea  
702 floor and causing mantle material to flow underneath the continents causing uplift (Tamisiea et al.,  
703 2014).

705 The uncertainty in projections of sea level rise at Singapore is substantially larger than for global  
706 mean projections, mainly due to the additional uncertainty associated with representation of regional  
707 oceanographic processes (the [oceanographicsteric/dynamic](#) contribution to sea level change) by the  
708 coarse resolution CMIP5 models. Scaling up of the ice sheet and glacier terms using the Slangen et  
709 al. (2014) fingerprints also contributed to the increased uncertainty of the regional projections. This  
710 increased uncertainty is larger for RCP8.5 than for RCP4.5. Over the first half of the 21st Century the  
711 projected rate of sea level rise is similar for both RCP4.5 and RCP8.5. Hence, on this timescale, sea  
712 level rise projections are largely independent of emissions [pathway-pathway](#), meaning the uncertainty  
713 range is dominated by methodological and model uncertainty. In both RCP4.5 and RCP8.5 there is a  
714 substantial acceleration in the rate of sea level rise over the 21st Century, particularly during the early  
715 and mid-periods of the 21<sup>st</sup> century. A simple linear extrapolation of observed long-term regional  
716 trends (as reported for Singapore by Tkalech et al., 2013) is therefore likely to grossly underestimate  
717 future sea level rise.

### 718 4.2 Surge changes

721 Time series of annual maximum skew surge at grid point 'a' from each of the four model simulations  
722 are presented in Figure 7. (NB. projected changes in surge and significant wave height both have  
723 very large spatial scales compared with the scale of Singapore. As a result, it was found that choice  
724 of model grid point did not significantly impact the results.) For consistency all skew surge and  
725 significant wave height results presented in this paper are taken from grid point 'a' (see Figure 1 for  
726 location). For each simulation a non-stationary GEV model fit to the annual maximum significant  
727 wave height time series was used to diagnose a linear century-scale trend in return level associated  
728 with any given return period. For each simulation the P value associated with the improvement in fit  
729 on moving from a stationary to a non-stationary GEV model is quoted in Figure 7. There is always  
730 some model improvement with a non-stationary fit because more parameters are added to the  
731 statistical model (i.e. a linear time-variation in both location and scale). Taking the CNRM model as  
732 an example, the P value is 77%, meaning the small amount of apparent non-stationarity in the CNRM  
733 data could easily arise by chance from random variations in stationary data. Thus we cannot discount  
734 our null hypothesis of stationarity in the CNRM data. The IPSL model, on the other hand, is consistent

with a visual assessment of the data. The P value is very small and we conclude that this data is unlikely to arise from a truly stationary process. Visually, there is a strong suggestion in the IPSL data of a reduction in interannual variability over the 21st century. The standard diagnostic of the quality of the fit of the stationary GEV distribution to the annual mean skew surge data for each simulation is included in Appendix A24 for each of the simulations. Projected century-scale trends in return level are reported in Table 4 and shown diagrammatically in Figure 8. Treating the four models as a small ensemble of equally plausible simulations, we obtain an ensemble [5%ile, 95%ile] of the diagnosed trend in the one hundred-year return level of [-63 , 30] mm/century. We do not find a statistically significant trend in skew surge for any of the return levels tested. Uncertainties in skew surge trends are small compared to the uncertainties in projected mean sea-level change of for example [450, 1020] mm (see Table 3) over the 21st century under RCP8.5. As no statistically significant trends in skew surge return levels are projected for RCP8.5, we would not expect to find trends for the less severe RCP4.5 scenario.

### 4.3 Wave changes

Time series of annual maximum significant wave height at grid point 'a' from each of the four simulations are presented in Figure 9. The standard diagnostic of the quality of the fit of the stationary GEV distribution to the significant wave height and annual maxima for each simulation is shown in the Appendix A3. All of the resulting projections of century-scale trends were small and negative, with the exception of the IPSL forced simulation for which a 35 mm century<sup>-1</sup> increase in the 2-year return level was obtained. The model ensemble of the diagnosed trend in 100-year significant wave height return level is [-0.73 , 0.29] mm century<sup>-1</sup>. Diagnosed trends in 2, 20, 100, 1000, and 10000-year return levels are given in Table 5 and presented diagrammatically in Figure 10. The small sample size of four climate models and the large spread in projections of century-scale change in significant wave height at long return periods means that we cannot rule out positive trends, even though the central estimates of the trends are small and negative in each of the four models.

## 5. Discussion

The overriding conclusion from this study is that change in time mean sea level will be the dominant process influencing the changing vulnerability of Singapore to coastal inundation over the 21<sup>st</sup> Century. Several studies have drawn similar conclusions for other parts of the world e.g. in the North Sea (Sterl et al., 2009), around the UK (Lowe et al., 2009) and globally (Bindoff et al., 2007). It is notable that the central estimates of sea level rise by 2100 (of 0.52 m and 0.74 m under the RCP4.5 and RCP8.5 scenarios respectively) are of similar magnitude to the most damaging surge events recorded at Singapore over recent decades (In describing extreme events occurring since the 1970s, Tkalic et al. (2009) report sea level anomalies ranging from 43 cm to ~60 cm). Hence Singapore is a country particularly vulnerable to sea level rise. Wong (1992) previously highlighted this vulnerability, noting that by adding 1 m to current chart datum levels at Singapore (comparable to our upper estimate of a 1.02 m sea level rise by 2100) the mean spring high water level of 3.8 m will be close to the highest recorded water level to date, of 3.9 m.

The climate simulations presented in this work suggest there will be no significant change in the frequency of extreme storm surge or wave events during the 21<sup>st</sup> century over and above that due to mean sea-level rise. Extreme events of the magnitude seen over recent decades will, however, have a much greater impact when superimposed on rising sea levels. Those involved in mitigating the

781 potential impacts of future climate change on Singapore's coastline therefore need to combine  
782 projections of sea level rise with skew surge return level data. Site specific projections of future  
783 extreme still water level can be obtained by linearly combining return levels derived from tide gauge  
784 data with the sea level change projections presented in Table 3. (Tide-gauge data represent the best  
785 information available about present-day location-specific return levels, however, it is worth noting that  
786 uncertainties in the present-day return levels derived from relatively short tide-gauge records are likely  
787 to be a large component of the combined uncertainty in projected future return-level curves.) In the  
788 longer term there is potential to develop better estimates of current risk by combining model-derived  
789 information with observed time series. The skew surge joint probability method (Batstone et al., 2013)  
790 provides an approach to addressing this problem.

791 ~~There are several caveats to the sea level, surge and wave projections presented in this study and we~~  
792 ~~consider each in turn in the following paragraphs. Mean sea level projections are presented as likely~~  
793 ~~(66-100% probability) ranges for the RCP4.5 and RCP8.5 scenarios of future greenhouse gas~~  
794 ~~concentrations, taking into account a number of uncertainties that cannot be formally quantified with~~  
795 ~~the present state of scientific knowledge. As noted previously, sea level projections do not account~~  
796 ~~for the unlikely event of a collapse of the marine-based sectors of the Antarctic ice sheet. There are~~  
797 ~~several caveats to the sea level, surge and wave projections presented in this study and we consider~~  
798 ~~each in turn in the following paragraphs. Mean sea level projections are presented as likely (66-100~~  
799 ~~% probability) ranges for the RCP4.5 and RCP8.5 climate change scenarios, taking into account a~~  
800 ~~number of uncertainties that cannot be robustly quantified with the present state of scientific~~  
801 ~~knowledge. We note that recent studies have attempted to provide information outside of the IPCC~~  
802 ~~likely range (Kopp et al., 2014 Jevrejeva et al., 2014) and this is an important topic of ongoing~~  
803 ~~discussion by the research community (Hinkel et al., 2015). As noted previously, our sea level~~  
804 ~~projections do not account for the unlikely event of a collapse of the marine-based sectors of the~~  
805 ~~Antarctic ice sheet.~~ Based on current understanding, AR5 assessed that such a collapse, if initiated,  
806 could cause global mean sea level to rise substantially above the given likely range during the 21st  
807 century. This potential additional contribution cannot be precisely quantified, but the AR5 report  
808 assessed with medium confidence that it would not exceed several tenths of a metre of sea level rise  
809 during the 21st century (Church et al, 2013). This remains one of the most important structural  
810 uncertainties in projecting sea level extremes. An additional source of uncertainty arises from taking  
811 patterns of change associated with land ice, land water and GIA from a single source (i.e. the maps  
812 generated by Slangen et al., 2014). While Slangen's data are considered very credible estimates  
813 based on current understanding, we do not include here any estimate of uncertainties in sea level  
814 change that could arise from using alternative estimates of these patterns. The CMIP5 models, due  
815 to their low resolution, have limited ability to represent meso-scale hydrographic processes important  
816 to regional dynamics. Previous studies (e.g. Lowe et al., 2009 and Perrette et al., 2013), suggest,  
817 however, that large-scale oceanic signals propagate freely into the coastal region, and are not overtly  
818 affected by the coarse resolution of the models. In common with previous studies (e.g. Lowe et al.,  
819 2009 and Perrette et al., 2013), we assume that large-scale oceanic signals propagate freely into the  
820 coastal region. The effects of anthropogenic disturbance such as resource extraction and land  
821 reclamation on sea level projections are also not considered in this work. Finally, it is important to  
822 note that the probability attributed to the sea level projections is calculated without accounting for the  
823 potential effects of future seismic activity; the only vertical land movement process considered in this  
824 study being glacial-isostatic adjustment. It is possible that vertical land movement associated with  
825 seismic activity may dominate changes in relative sea level over decadal time scales. The Earth  
826 Observatory of Singapore state that:

"Sea level could rise faster than the IPCC predicted after a big earthquake on the Sunda Megathrust. This is due to the overall tectonics of the region. After a big earthquake on the megathrust, the whole Sunda shelf will experience a subsidence."  
(<http://www.earthobservatory.sg/faq-on-earth-sciences/singapore-threatened-earthquakes-0>).

There are a number of further caveats associated with the modelling of extreme events. Waves and surge have been modelled separately, meaning wave-surge interactions are not accounted for. Surge propagation from outside the boundaries of the surge model domain is also not considered (except by application of a static inverse barometer effect at the boundaries). Over shallow seas, however, wind is the dominant factor in surge generation, suggesting that surge propagation from outside the boundaries will not be a dominant factor in driving extreme water levels on the Sunda shelf (Horsburgh and Wilson, 2007). The impacts of changes in mean water depth on tidal resonance and on surge propagation are also not considered in this work. Pickering (2014) investigated the impact on tidal dynamics of raising GMSL by 2 m and found a change in mean high water level of the order 10 cm around Singapore. Howard et al. (2010), Sterl et al. (2009), and Lowe et al. (2001) find in studies of the northwest European shelf that changing the water depth affects the time of arrival of a storm surge, but not the surge height. Hence, we suggest that any impact of rising sea levels on tidal dynamics will be small compared to sea level rise. Finally, our simulations assume a fixed coastline with no inundation. Further work with a high resolution inundation model is required to understand the land area at risk from inundation due to sea level rise, and to design appropriate coastal defences to best mitigate this risk.

## 6. Conclusions

Regional projections of changes in long-term mean sea level and in the frequency of extreme storm surge and wave events over the 21st century have been generated for Singapore. Local changes in time mean sea level were evaluated using the process-based climate model data and methods presented in the IPCC AR5. Regional surge and wave forecast simulations extending from 1970 to 2100 were generated using high resolution (~12 km) regional surge (Nucleus for European Modelling of the Ocean - NEMO) and wave (WaveWatchIII) models. Ocean simulations were forced by four regional atmospheric model solutions, which were in turn nested within global atmospheric simulations generated for the IPCC AR4. The four climate models were chosen to best represent historical conditions and included the GFDL-CM3 model which exhibited the largest area-averaged changes in 850 hPa wind speeds during both the SW and NE monsoon seasons. An additional atmospheric regional model simulation driven by a global atmospheric reanalysis was used to force historical regional ocean model simulations extending from 1980-2010. The hindcast simulation was used to demonstrate the skill of the models in simulating regional tides and surge events (through comparison to tide gauge data) and significant wave heights (through comparison to satellite altimetry data).

Central estimates of long-term mean sea level rise at Singapore by 2100 are projected to be 0.52 m (0.74 m) under the RCP 4.5(8.5) scenarios respectively. These values are very close to the global mean estimates presented in the IPCC AR5. Sea level rise at Singapore resulting from mass loss from ice sheets and glaciers is projected to be 10-15% larger than the global mean. This will, however, be offset by elevation of the land mass due to glacial isostatic adjustment. The likely ranges of projected sea level rise at Singapore are substantially larger than the global mean projections, mainly due to the uncertainty associated with representation of regional oceanographic processes by the coarse resolution CMIP5 models. Due to an acceleration in the rate of sea level rise throughout the early and mid-21<sup>st</sup> century, extrapolation of long-term tide-gauge records does not provide

873 reliable estimates of future sea level change and systematically underestimates the magnitude of  
874 future sea level rise for both scenarios.

875 The [5%ile, 95%ile] of diagnosed trend in one hundred-year skew surge return level, obtained by  
876 treating the four models as a small ensemble of equally plausible simulations is  
877 [-63, 30] mm century<sup>-1</sup>. The corresponding [5%ile, 95%ile] of the diagnosed trend in one hundred-  
878 year significant wave height return level is [-0.73, 0.29] mm century<sup>-1</sup>. The uncertainties in projected  
879 century-scale trend in skew surge and significant wave height are small compared to the uncertainties  
880 in projected mean sea-level change of for example [450, 1020] mm over the 21st century under  
881 RCP8.5. We find no statistically significant changes in extreme skew surge events and no statistically  
882 significant changes in extreme significant wave height under the RCP 8.5 scenario over and above  
883 that due to mean sea-level change using the four model ensembles. Our primary finding is then that  
884 change in time mean sea level will be the dominant process influencing the changing vulnerability of  
885 Singapore to coastal inundation over the 21st Century. We note that the largest recorded surge  
886 residual in the Singapore Strait of ~84 cm (Tklich et al., 2009) lies between the central and upper  
887 estimates of sea level rise by 2100.

888

## 889 Acknowledgements

890 This study was carried out as part of Singapore's Second National Climate Change Study and was  
891 funded by the government of Singapore. Full reports of the study can be found of the Centre for  
892 Climate Research Singapore (CCRS) website at [http://ccrs.weather.gov.sg/publications-second-](http://ccrs.weather.gov.sg/publications-second-National-Climate-Change-Study-Science-Reports)  
893 [National-Climate-Change-Study-Science-Reports](http://ccrs.weather.gov.sg/publications-second-National-Climate-Change-Study-Science-Reports).

894 Jamie Kettleborough and Ian Edmond provided scripts for downloading and archiving the CMIP5 data  
895 used in this study. We thank Aimée Slangen for providing spatial fingerprint data used in the  
896 projections of regional sea level change and Mark Carson for assistance with carrying out the  
897 comparison with the Slangen et al (2014) ~~oceanographic~~<sup>steric/dynamic</sup> sea level changes. We  
898 acknowledge use of the MONSooN system, a collaborative facility supplied under the Joint Weather  
899 and Climate Research Programme, which is a strategic partnership between the Met Office and the  
900 Natural Environment Research Council. This work also used the ARCHER UK National  
901 Supercomputing Service (<http://www.archer.ac.uk>).

902

## 903 References

- 904 Allen, J.-I., Aiken, J., Anderson, T.R., Buitenhuis, E., Cornell, S., Geider, R., Haines, K., Hirata, T.,  
905 Holt, J., Le Quéré, C., Hardman-Mountford, N., Ross, O.N., Sinha, B., While, J., (2010). Marine  
906 ecosystem models for earth systems applications: the MarQUEST experience. *Journal of Marine*  
907 *Systems*, 81, 19–33.
- 908
- 909 Atlas R, Hoffman RN, Ardizzone J, Leidner SM, Jusem JC, Smith DK, Gombos D (2011) A cross-  
910 calibrated, multiplatform ocean surface wind velocity product for meteorological and oceanographic  
911 applications. *Bull. Amer. Meteor. Soc.*, 92:157-174. doi: 10.1175/2010BAMS2946.1
- 912 Batstone C, Lawless M, Tawn J, Horsburgh K, Blackman D, McMillan A, Worth D, Laeger S, Hunt T  
913 (2013) A UK best-practice approach for extreme sea-level analysis along complex topographic  
914 coastlines. *Ocean Engineering*, 71:28-39. 10.1016/j.oceaneng.2013.02.003



915 Bidlot JR, Holmes-Bell DJ, Wittmann PA, Lalbeharry R, Chen HS (2000) Intercomparison of the  
 916 performance of operational ocean wave forecasting systems with buoy data. European Centre for  
 917 Medium-Range Weather Forecasts (ECMWF) Technical Memorandum Number 315 also 2002,  
 918 Weather and Forecasting, 17:287-310.

919 Bidlot JR, Li LG, Wittmann P, Fauchon M, Chen H, Lefevre JM, Bruns T, Greenslade D, Arduin F,  
 920 Kohno N, Park S, Gomez M (2007) Inter-comparison of operational wave forecasting systems. 10th  
 921 International Workshop on Wave Hindcasting and Forecasting and Coastal Hazard Symposium, North  
 922 Shore, Oahu, Hawaii, 11-16 November 2007.

923 Bidlot JR, Holt MW (2006) Verification of operational global and regional wave forecasting systems  
 924 against measurements from moored buoys. JCOMM Technical Report, 30. WMO/TDNo.1333.

925 Bindoff NL, Willebrand J, Artale V, Cazenave A, Gregory J, Gulev S, Hanawa K, Le Quéré C, Levitus  
 926 S, Nojiri Y, Shum CK, Talley LD, Unnikrishnan A (2007) Observations: Oceanic Climate Change and  
 927 Sea Level. In: Climate Change 2007: The Physical Science Basis. Contribution of Working Group I to  
 928 the Fourth Assessment Report of the Intergovernmental Panel on Climate Change [Solomon S, Qin  
 929 D, Manning M, Chen Z, Marquis M, Averyt KB, Tignor M, Miller HL (eds.)]. Cambridge University  
 930 Press, Cambridge, United Kingdom and New York, NY, USA.

931 [Bird MI, Austin WEN, Wurster CM, et al. Punctuated eustatic sea-level rise in the early mid-Holocene. Geology. 2010;38:803–6. doi:10.1130/G31066.1](#)  
 932

933 Church JA, et al. (2013) Sea Level Change. In: Climate Change 2013: The Physical Science Basis.  
 934 Contribution of Working Group I to the Fifth Assessment Report of the Intergovernmental Panel on  
 935 Climate Change [Stocker TF, Qin D, Plattner GK, Tignor M, Allen SK, Boschung J, Nauels A, Xia Y,  
 936 Bex V, Midgley PM (eds.)]. Cambridge University Press, Cambridge, United Kingdom and New York,  
 937 NY, USA.

938 Church JA, et al. (2001) Changes in sea level. In: Climate Change 2001: The Scientific Basis.  
 939 Contribution of Working Group I to the Third Assessment Report of the Intergovernmental Panel on  
 940 Climate Change [Houghton JT, et al. (eds.)]. Cambridge University Press, Cambridge, United  
 941 Kingdom and New York, NY, USA, pp. 639–693.

942 Coles S (2001) An introduction to statistical modeling of extreme values. pp 208. London: Springer,  
 943 2001.

944 Dee DP, Uppala SM, Simmons AJ, Berrisford P, Poli P, Kobayashi S, Andrae U, Balmaseda M A,  
 945 Balsamo G, Bauer P, Bechtold P, Beljaars ACM, van de Berg L, Bidlot J, Bormann N, Delsol C,  
 946 Dragani R, Fuentes M, Geer AJ, Haimberger L, Healy SB, Hersbach H, Hólm EV, Isaksen L, Kållberg  
 947 P, Köhler M, Matricardi M, McNally AP, Monge-Sanz BM, Morcrette JJ, Park BK, Peubey C, de  
 948 Rosnay P, Tavolato C, Thépaut JN, Vitart F (2011), The ERA-Interim reanalysis: configuration and  
 949 performance of the data assimilation system. Q.J.R. Meteorol. Soc., 137: 553–597. doi:  
 950 10.1002/qj.828

951 [de Vries H, Breton M, de Mulder T, Krestenitis Y, Ozer J, Proctor R, Ruddick K, Saloman JC, Voorrips A \(1995\) A comparison of 2D storm-surge models applied to three shallow European seas. Environmental Software, 10\(1\):23-42.](#)  
 952  
 953

954 [Hinkel J, Jaeger C, Nicholls RJ, Lowe J, Renn O, Peijun S \(2015\): Sea-level rise scenarios and coastal risk management, Nature Climate Change, 5, 188–190 \(2015\) doi:10.1038/nclimate2505.](#)  
 955



956 Horsburgh KJ, Wilson, C (2007) Tide-surge interaction and its role in the distribution of surge  
 957 residuals in the North Sea. *Journal of Geophysical Research*, 112 (C8). Art. No. C08003.  
 958 10.1029/2006JC004033.

959 Hosking JRM, Wallis JR, Wood EF (1985) Estimation of the generalized extreme-value distribution by  
 960 the method of probability-weighted moments. *Technometrics* 27(3):251-261.

961 Howard T, Lowe J, Horsburgh K (2010) Interpreting century-scale changes in southern North Sea  
 962 storm surge climate derived from coupled model simulations. *Journal of Climate* 23(23):6234-6247.

963 Howard T, Pardaens AK, Bamber JL, Ridley J, Spada G, Hurkmans RTWL, Lowe JA, Vaughan D  
 964 (2014) Sources of 21st century regional sea-level rise along the coast of northwest Europe, *Ocean*  
 965 *Sci.*, 10:473-483, doi: 10.5194/os-10-473-2014.

966 Huerta G, Bruno S (2007) Time-varying models for extreme values. *Environmental and Ecological*  
 967 *Statistics* 14(3):285-299.

968 IPCC AR4 (2007) Climate change 2007. The physical science basis. Summary for policymakers. In:  
 969 Alley R, Berntsen T, Bindoff NL, et al. (Eds.), *Contribution of Working Group I to the Fourth*  
 970 *Assessment Report of the Intergovernmental Panel on Climate Change*.

971 Kotz S, Nadarajah S (2000) *Extreme Value Distributions: Theory and Applications*. London: Imperial  
 972 College Press, 2000.

973 [Kopp RE, Horton RM, Little CM, Mitrovica JX, Oppenheimer M, Rasmussen DJ, Strauss BH, Tebaldi](#)  
 974 [C \(2014\) Probabilistic 21st and 22nd century sea-level projections at a global network of tide-gauge](#)  
 975 [sites. \*Earth's future\*. 2\(8\), 383-406.](#)

976 Lowe JA, Howard TP, Pardaens A, Tinker J, Holt J, Wakelin S, Milne G, Leake J, Wolf J, Horsburgh  
 977 K, Reeder T, Jenkins G, Ridley J, Dye S, Bradley S (2009) UK Climate Projections science report:  
 978 Marine and coastal projections. Met Office Hadley Centre, Exeter, UK.

979 Lowe JA, Gregory J, Flather R (2001) Changes in the occurrence of storm surges around the United  
 980 Kingdom under a future climate scenario using a dynamic storm surge model driven by the Hadley  
 981 Centre climate models. *Clim. Dynam.*, 18 (3-4):179–188.

982 [Madec G \(2008\) NEMO reference manual 3.4 STABLE : "NEMO ocean engine". Note du Pôle de](#)  
 983 [modélisation, Institut Pierre-Simon Laplace \(IPSL\), France, No 27 ISSN No 1288-1619.](#)

984 [Maren DV, Gerritsen H \(2012\) Residual flow and tidal asymmetry in the Singapore Strait, with](#)  
 985 [implications for resuspension and residual transport of sediment. \*Journal of Geophysical Research\*,](#)  
 986 [117, C04021, doi:10.1029/2011JC007615.](#)

987 McSweeney C, Rahmat R, Redmond G, Marzin C, Murphy J, Jones R, Cheong WK, Lim SY, Sun X  
 988 (2015) Singapore's Second National Climate Change Study – Phase 1: Chapter 3: Sub-selection of  
 989 CMIP5 GCMs for downscaling over Singapore. [Web link: [http://ccrs.weather.gov.sg/publications-](http://ccrs.weather.gov.sg/publications-second-National-Climate-Change-Study-Science-Reports)  
 990 [second-National-Climate-Change-Study-Science-Reports](http://ccrs.weather.gov.sg/publications-second-National-Climate-Change-Study-Science-Reports)]

991 McSweeney CF, Jones RG, Lee RW, Rowell DP (2015) Selecting CMIP5 GCMs for downscaling  
 992 over multiple regions. *Climate Dynamics*, 44:3237-3260.

993 Mendez FJ, Menendez M, Luceo A, Losada IJ (2008) Estimation of the long-term variability of  
 994 extreme significant wave height using a time-dependent Peak Over Threshold (POT) model, *J.*  
 995 *Geophys. Res.*, 111:C07024, doi:10.1029/2005JC003344.

996 Méndez FJ, Menéndez M, Luceño A, Losada IJ (2007) Analyzing Monthly Extreme Sea Levels with a  
997 Time-Dependent GEV Model. *J. Atmos. Oceanic Technol.*, 24:894–911. doi:  
998 <http://dx.doi.org/10.1175/JTECH2009.1>

999 Meinshausen M, Smith SJ, Calvin KV, Daniel JS, Kainuma MLT, Lamarque JF, Matsumoto K, S.  
1000 Montzka SA, Raper SCB, Riahi K, Thomson AM, Velders GJM van Vuuren D (2011) The RCP  
1001 Greenhouse Gas Concentrations and their Extension from 1765 to 2300. *Climatic Change* (Special  
1002 Issue), DOI: 10.1007/s10584-011-0156-z.

1003 Monbaliu J et al. (2000) "The spectral wave model, WAM, adapted for applications with high spatial  
1004 resolution." *Coastal engineering* 41(1):41-62.

1005 Mousavi M, Irish J, Frey A, Olivera F, Edge B (2011) Global warming and hurricanes: The potential  
1006 impact of hurricane intensification and sea level rise on coastal flooding. *Clim. Change*, 104:575–597.

1007 Pardaens A, Gregory, JM Lowe, J (2011) A model study of factors influencing projected changes in  
1008 regional sea level over the twenty-first century. *Clim. Dyn.*, 36:2015–2033.

1009 Pawlowicz R, Beardsley B, Lentz S (2002) Classical Tidal Harmonic Analysis Including Error  
1010 Estimates in MATLAB using T\_TIDE", *Computers and Geosciences*, 28:929-937.

1011 Peltier WR (2004) Global Glacial Isostasy and the Surface of the Ice-Age Earth: The ICE-5G (VM2)  
1012 Model and GRACE, *Ann. Rev. Earth and Planet. Sci.*, 32, 111-149.

1013 [Penduff T, Juza M, Brodeau L, Smith GC, Barnier B, Molines JM, Treguier AM, Madec G \(2010\)](#)  
1014 [Impact of global ocean model resolution on sea-level variability with emphasis on interannual time](#)  
1015 [scales. \*Ocean Science\*, 6, 269–284.](#)

1016

1017 Perrette, M., Landerer, F., Riva, R., Frieler, K., and Meinshausen, M (2013), A scaling approach to  
1018 project regional sea level rise and its uncertainties. *Earth System Dynamics*, 4(1), 11–29.  
1019 doi:10.5194/esd-4-11-2013

1020 Pickering M (2014) The impact of future sea-level rise on the tides. University of Southampton, Ocean  
1021 and Earth Science, Doctoral Thesis , 347pp.

1022 Slangen ABA, Carson M, Katsman, CA, van de Wal RSW, Koehl A, Vermeersen, LLA Stammer D  
1023 (2014) Projecting twenty-first century regional sea-level changes, *Climatic Change*, doi:  
1024 10.1007/s10584-014-1080-9.

1025 [Jevrejeva S, Grinsted A, Moore CJ \(2014\) Upper limit for sea level projections by 2100.](#)  
1026 [\*Environmental Research letters\*, 9, 1-9.](#)

1027 Smith JM, Cialone MA Wamsley TV McAlpin TO (2010) Potential impact of sea level rise on coastal  
1028 surges in southeast Louisiana. *Ocean Eng.*, 37:37–47.

1029 Sterl A, van den Brink H, de Vries H, Haarsma R, van Meijgaard E (2009) An ensemble study of  
1030 extreme North Sea storm surges in a changing climate. *Ocean Sci.*, 5:369–378.

1031 Tamisiea ME, Mitrovica JX (2011) The moving boundaries of sea level change: Understanding the  
1032 origins of geographic variability. *Oceanography* 24(2):24–39, doi:10.5670/oceanog.2011.25.

1033 Tamisiea ME, Hughes CW, Williams SDP, Bingley RM (2014) Sea level: measuring the bounding  
1034 surfaces of the ocean. *Philosophical Transactions of the Royal Society of London, A*, 372: 2025.  
1035 20130336. 10.1098/rsta.2013.0336

1036 Tkalic, P, Vethamony P, Babu MT, Pokratath R (2009) Seasonal sea level variability and anomalies  
 1037 in the Singapore Strait. Proceedings of International Conference in Ocean Engineering, ICOE 2009  
 1038 IIT Madras, Chennai, India. 1-5 Feb. 2009

1039 Tkalic P, Vethamony P, Luu QH, Babu MT (2013), Sea level trend and variability in the Singapore  
 1040 Strait, Ocean Sci., 9, 293-300, doi:10.5194/os-9-293-2013.

1041 Tolman HL (1997) User manual and system documentation of WAVEWATCH-III version 1.15. NOAA /  
 1042 NWS / NCEP / OMB Technical Note 151, 97 pp.

1043 Tolman HL (1999) User manual and system documentation of WAVEWATCH-III version 1.18. NOAA  
 1044 / NWS / NCEP / OMB Technical Note 166, 110 pp.

1045 Tolman HL (2009) User manual and system documentation of WAVEWATCH III version 3.14. NOAA /  
 1046 NWS / NCEP / MMAB Technical Note 276, 194 pp.

1047 Tolman HL, Chalikov, DV (1996) Source terms in a 3rd generation wind-wave model. J. Phys.  
 1048 Oceanogr., 26:2497-2518.

1049 Wilby R L, Troni J, Biot Y, Tedd L, Hewitson BC, Smith DM, Sutton RT (2009), A review of climate risk  
 1050 information for adaptation and development planning, International Journal of Climatology,  
 1051 29(9):1193-1215.

1052 Whetton P, Hennessy K, Clarke J, McInnes K, Kent K (2012) Use of Representative Climate Futures  
 1053 in impact and adaptation assessment, Climatic Change, 115(3-4):433-442.

1054 Wong PP (1992) Impact of a sea level rise on the coasts of Singapore: preliminary observations  
 1055 Journal of Southeast Asian Earth Sciences, Vol. 7, No. 1, pp. 65-70, 1992.

1056

1057

1058

1059

1060

1061

1062

1063

1064

1065

1066

1067

1068  
1069  
1070  
1071  
1072  
1073  
1074  
  
  
  
1075  
  
1076  
  
1077  
1078  
1079

Tables

**Table 1:** Summary table of methodologies employed to estimate the different components of sea level rise at Singapore, including scaling factors used to convert global mean trends into local trends.

Component	Methodology
1. <a href="#">Oceanographic</a> Steric/dynamic sea level	CMIP5 climate model estimates of global thermal expansion and dynamic sea level are combined for each model. Differences between the two periods 1986-2005 and 2081-2100 are computed for each climate change scenario. A multi-model mean and spread in this component is extracted for Singapore using a nearest-neighbour approach. Time series are constructed based on the assumption that the change signal emerges proportionally to AR5 estimates of global thermal expansion.
2. Glaciers	Time series of global sea level rise from AR5 data files are scaled by a factor of 1.11, according to the spatial fingerprint information provided by Slangen et al. (2014).
3. Greenland surface mass balance	Time series of global sea level rise from AR5 data files are scaled by a factor of 1.14, according to the spatial fingerprint information provided by Slangen et al. (2014).
4. Antarctica surface mass balance	Time series of global sea level rise from AR5 data files are scaled by a factor of 1.13, according to the spatial fingerprint information provided by Slangen et al. (2014).
5. Greenland dynamics	Time series of global sea level rise from AR5 data files are scaled by a factor of 1.16, according to the spatial fingerprint information provided by Slangen et al. (2014).
6. Antarctica dynamics	Time series of global sea level rise from AR5 data files are scaled by a factor of 1.19, according to the spatial fingerprint information provided by Slangen et al. (2014).
7. Land water storage	Time series of global sea level rise from AR5 data files are scaled by a factor of 0.81, according to the spatial fingerprint information provided by Slangen et al. (2014).
8. Glacial isostatic adjustment (GIA)	Estimate based on ICE5G (Peltier, 2004) model as provided by Slangen et al. (2014).
9. Inverse barometer	Assessed from AR5 supplementary data files. Not included in projections, given the negligible contribution.

1080

1081

1082 **Table 2:** Median values and *likely* (in IPCC calibrated language – see section 2.1) ranges (square  
 1083 brackets) for projections of time mean sea level rise and its contribution in metres for 2081-2100  
 1084 relative to 1986-2005 for Singapore and the global average (as reported in Table 13.5 of AR5, Church  
 1085 et al., 2013).  
 1086

Sea level component	RCP4.5 change (m)		RCP8.5 change (m)	
	Singapore	Global	Singapore	Global
Expansion / Oceanographic Steric/Dynamic	0.20 [0.12,0.27]	0.19 [0.14,0.23]	0.27 [0.18,0.36]	0.27 [0.21,0.33]
Glaciers	0.14 [0.07,0.22]	0.12 [0.06,0.19]	0.18 [0.10,0.26]	0.16 [0.09,0.23]
Greenland Surface Mass Balance	0.05 [0.01,0.18]	0.04 [0.01,0.09]	0.08 [0.03,0.18]	0.07 [0.03,0.16]
Antarctica Surface Mass Balance	-0.02 [-0.06,-0.01]	-0.02 [-0.05,-0.01]	-0.05 [-0.08,-0.01]	-0.04 [-0.07,-0.01]
Greenland Dynamics	0.05 [0.01,0.07]	0.04 [0.01,0.06]	0.06 [0.02,0.08]	0.05 [0.02,0.07]
Antarctica Dynamics	0.08 [-0.01,0.19]	0.07 [-0.01,0.16]	0.08 [-0.01,0.19]	0.07 [-0.01,0.16]
Land Water	0.03 [-0.01,0.07]	0.04 [-0.01,0.09]	0.03 [-0.01,0.07]	0.04 [-0.01,0.09]
GIA	-0.03	N/A	-0.03	N/A

1087

1088

1089 **Table 3:** Estimates of global sea level rise from the IPCC AR5 (Church et al., 2013) alongside our  
 1090 regional estimates for Singapore. Following the definitions in AR5, there is a 66-100% chance that  
 1091 future sea level rise will fall within the ranges quoted. Based on current understanding, only the  
 1092 collapse of marine-based sectors of the Antarctic ice sheet, if initiated, could cause global mean sea  
 1093 level to rise substantially above the *likely* range during the 21st century. This potential additional  
 1094 contribution cannot be precisely quantified but there is medium confidence that it would not exceed  
 1095 several tenths of a meter of sea level rise during the 21st century (Church et al, 2013).

1096

Scenario		2050			2100		
		Central	Lower	Upper	Central	Lower	Upper
RCP4.5	Global	0.23	0.17	0.29	0.53	0.36	0.71
	Singapore	0.22	0.14	0.29	0.52	0.29	0.73
RCP8.5	Global	0.25	0.19	0.32	0.74	0.52	0.98
	Singapore	0.25	0.17	0.32	0.74	0.45	1.02

1097

1098

1099  
1100  
1101  
1102  
1103  
1104  
  
1105  
1106  
1107  
1108  
  
1109  
1110  
1111  
1112  
1113  
1114  
1115  
1116  
1117

**Table 4:** Projected century-scale trends in skew surge for five return periods (excluding mean sea level change). Units are mmetres per century.

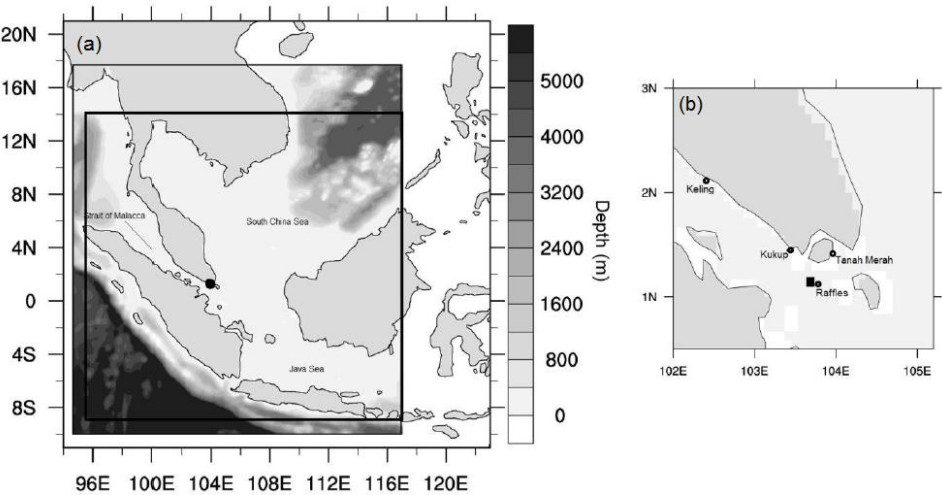
Period/years	2	20	100	1000	10000
Lower	-0.020	-0.040	-0.063	-0.090	-0.120
Central	0.00	-0.010	-0.020	-0.020	-0.030
Upper	0.020	0.020	0.030	0.050	0.060

**Table 5:** Projected century-scale trends in significant wave height for five return periods due to storminess changes (mmetres per century, to two decimal places).

Period/years	2	20	100	1000	10000
Lower	-0.15	-0.460	-0.730	-1.260	-2.030
Central	-0.030	-0.140	-0.220	-0.390	-0.620
Upper	0.080	0.190	0.290	0.490	0.780

1118 **Figures**

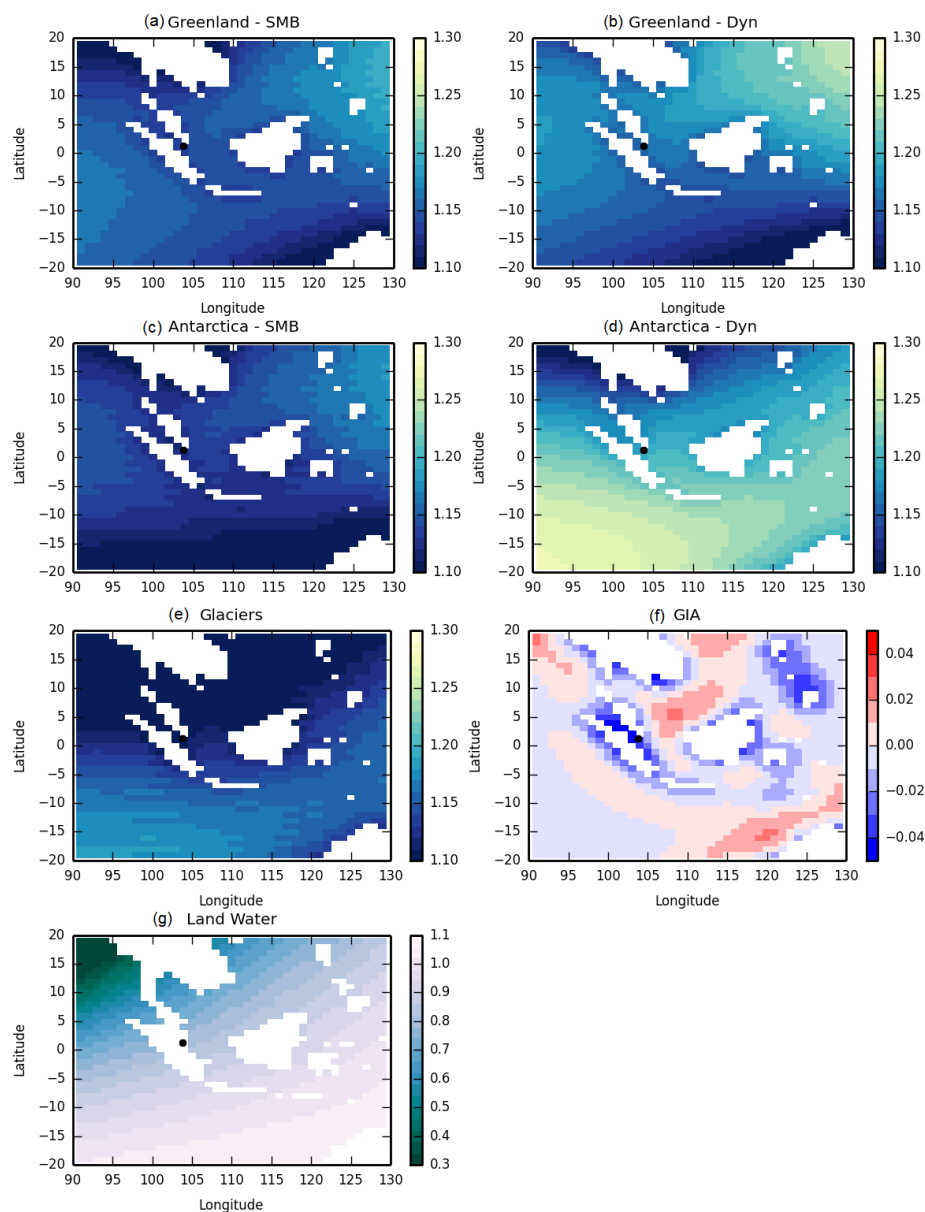
1119



1120

1121 **Figure 1:** (a) Bathymetric map showing the location of Singapore (black circle) in relation to  
1122 the climate model domain (outermost square), the surge model domain (shaded depth  
1123 contours), and the wave model domain (innermost square). (b) Map of Singapore showing  
1124 the location of tide gauge meters utilised for model validation, and showing the location of  
1125 grid point 'a' as referred to in the results section (black rectangle).

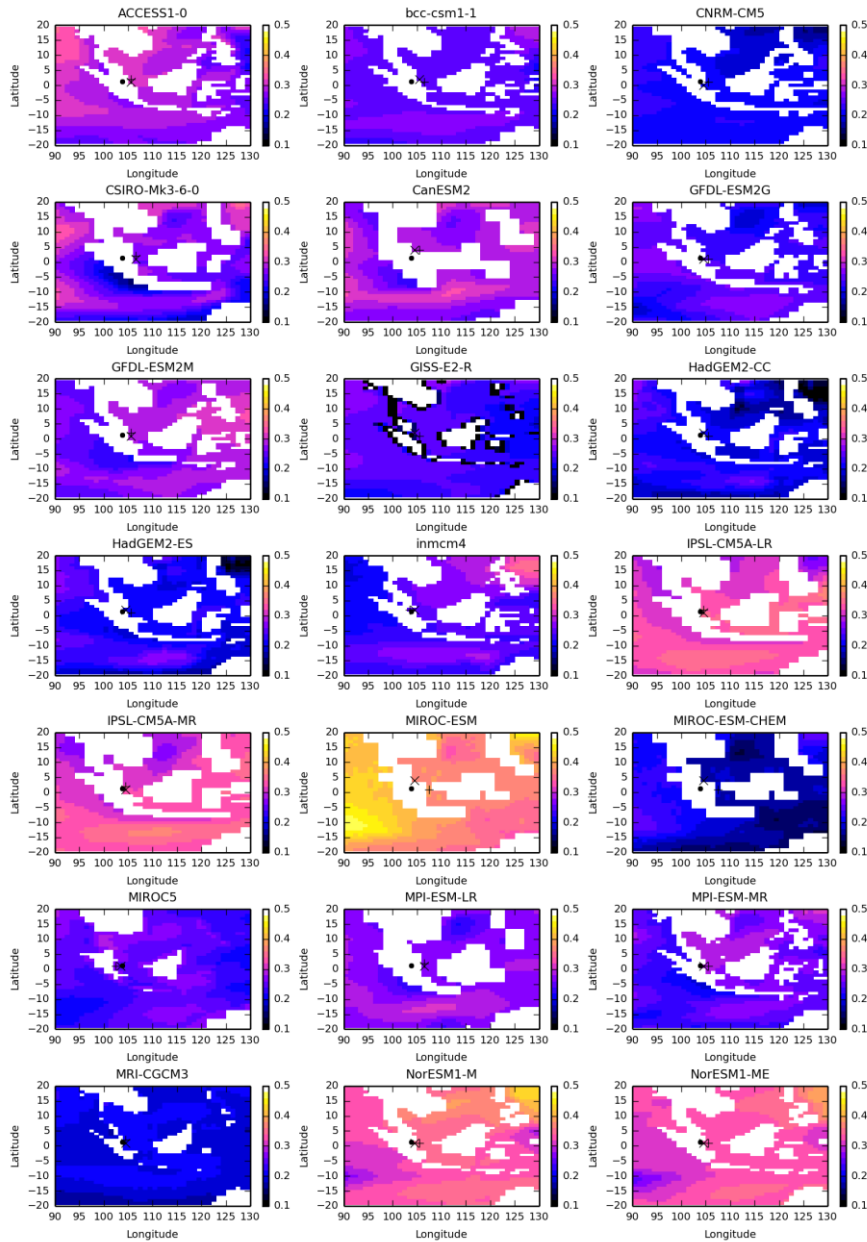
1126



1127

1128 **Figure 2:** Spatial fingerprints for changes in (a) Greenland surface mass balance, (b)  
 1129 Greenland dynamical change, (c) Antarctica surface mass balance, (d) Antarctica dynamical  
 1130 change, (e) glaciers, (f) glacial isostatic adjustment and (g) changes in land water use. Panels  
 1131 a-e represent the ratio of local relative sea level change per unit of GMSL rise associated with  
 1132 mass input to the oceans. The location of Singapore is shown by the black circle.  
 1133 Source: Slangen *et al.* (2014).

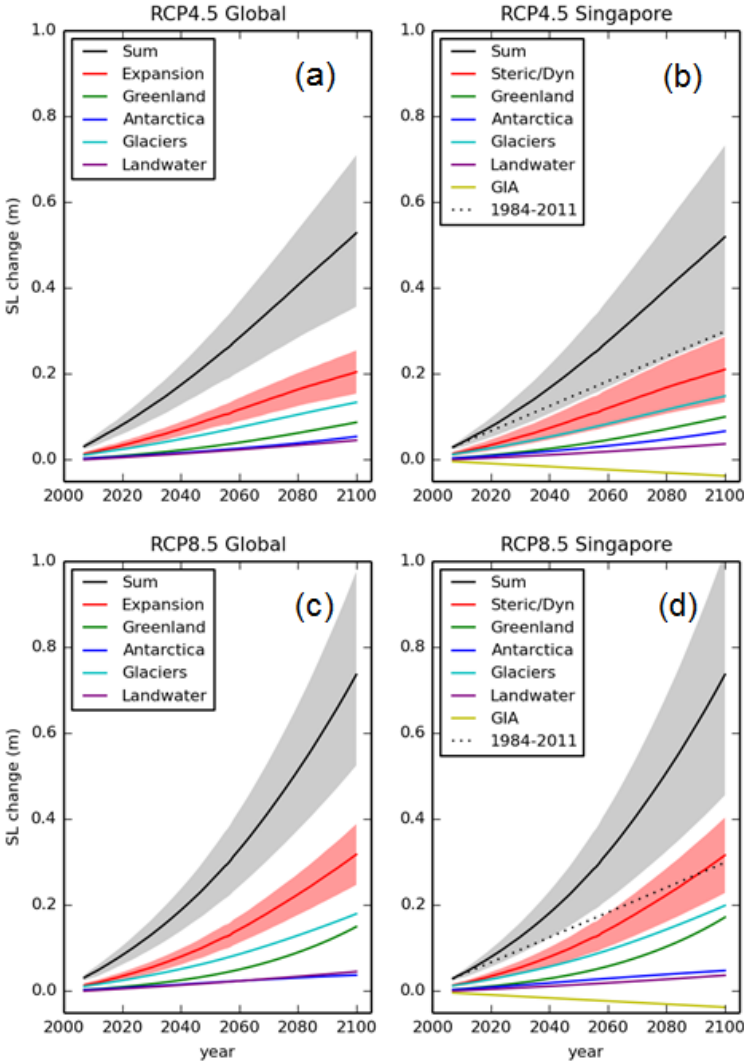




1134

1135 **Figure 3:** Projections of steric/dynamic sea level rise (metres) for 21 CMIP5 models under  
 1136 RCP8.5, computed as the difference between 1986-2005 and 2081-2100. The location of  
 1137 Singapore is shown by the black circle. The primary and secondary grid boxes used to extract  
 1138 time mean sea level for Singapore are shown by an x and +, respectively. Note the grid box  
 1139 selections for GISS-E2-R are away from potential problem areas for the land mask.

1140



1141

1142 **Figure 4:** Projections of sea level rise relative to 1986-2005 and its contributions as a  
1143 function of time for (a) global mean sea level (RCP4.5), (b) Singapore region (RCP4.5), (c)  
1144 global mean sea level (RCP8.5) and (d) Singapore region (RCP8.5). Lines show the median  
1145 projections. The likely ranges for the total and thermal expansion or steric/dynamic sea level  
1146 changes are shown by the shaded regions. The contributions from ice sheets include the  
1147 contributions from ice sheet rapid dynamical change. The dotted line shows an  
1148 extrapolation of the observed 1984-2011 rate of sea level change for the Singapore Strait  
1149 reported by Tkalich et al. (2013).

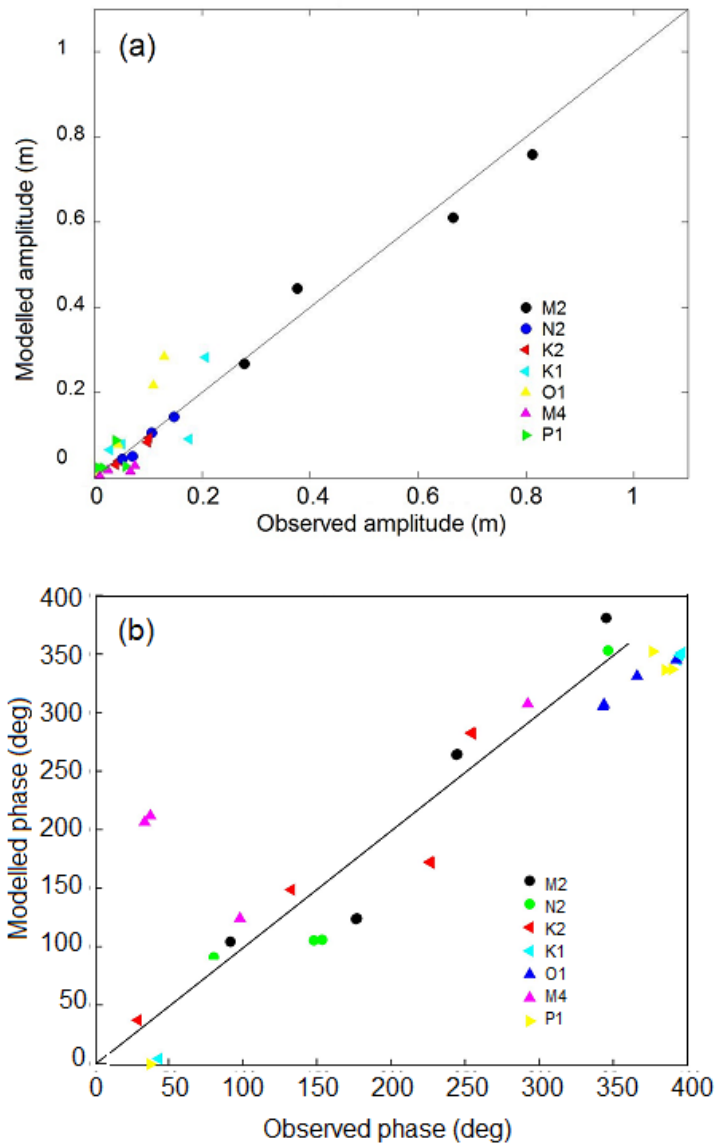
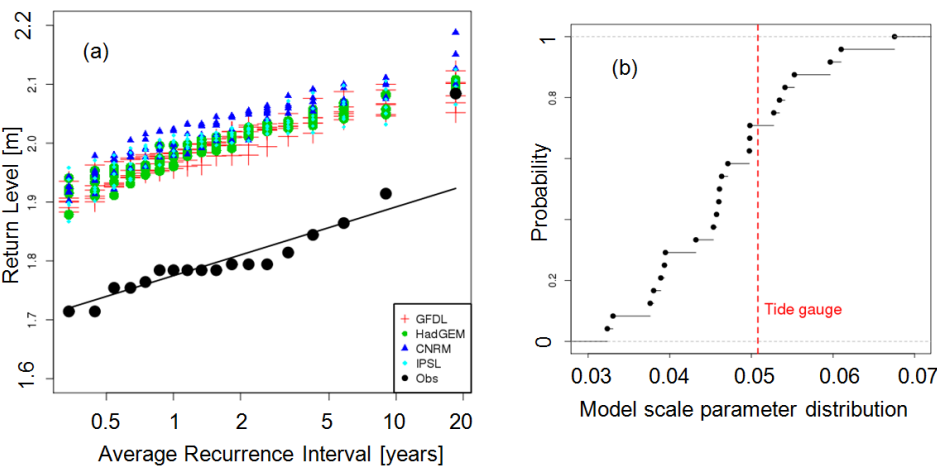


**Figure 5:** Comparison of modelled and observed (a) tidal amplitude and (b) tidal phase at 4 tide gauge stations close to Singapore (Keling, Tanah Merah, Raffles lighthouse and Kukup) station locations are marked in Figure 1.

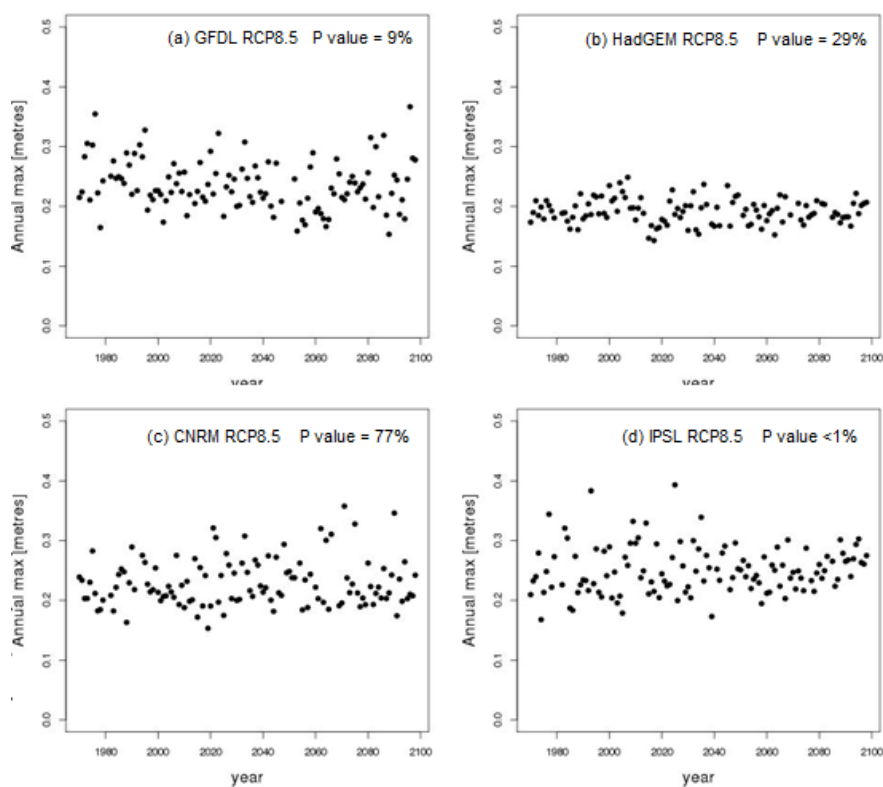
1156



1157

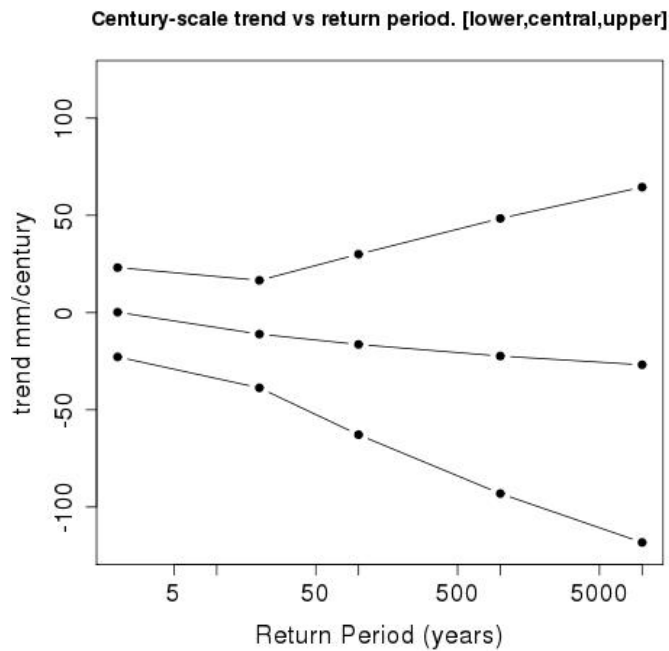
1158 **Figure 6:** (a) Empirical return level data of extreme water level based on 18 years of tide  
1159 gauge data from Raffles Light House (1996-2013), and 18-year long samples from the model  
1160 simulations at grid point 'a'. The fitted Gumbel distribution of the observations is shown by  
1161 the straight line. (b) Empirical cumulative density function of the scale parameters of the  
1162 model samples, showing that the scale parameter of the tide gauge data sits well within the  
1163 model distribution.

1164



1165

1166 **Figure 7:** Annual maxima skew surge obtained from the (a) GFDL, (b) HadGEM, (c) CNRM,  
 1167 and (d) IPSL forced simulations. The P value indicates the statistical significance of the  
 1168 improvement in fit when using a non-stationary GEV model: a large P value indicates little  
 1169 improvement; a small P value indicates significant improvement.



1170

1171

1172 **Figure 8:** Projected century-scale trends in skew surge for five return periods due to  
 1173 storminess changes only (i.e. excluding mean sea level change) (mm per century). Central,  
 1174 lower and upper estimates are shown.

1175

1176

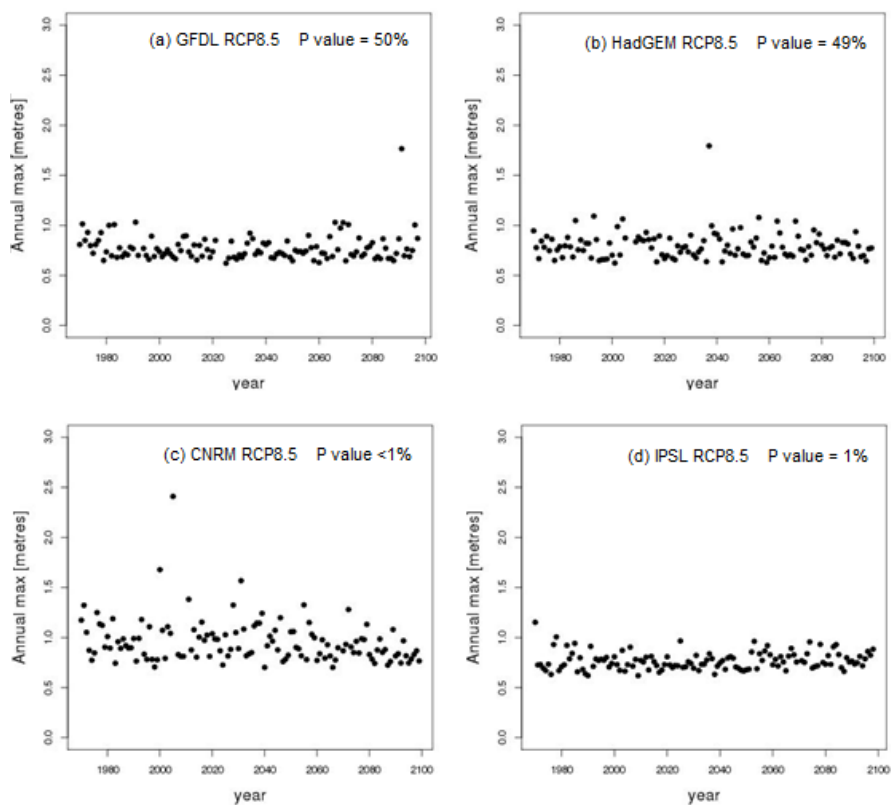
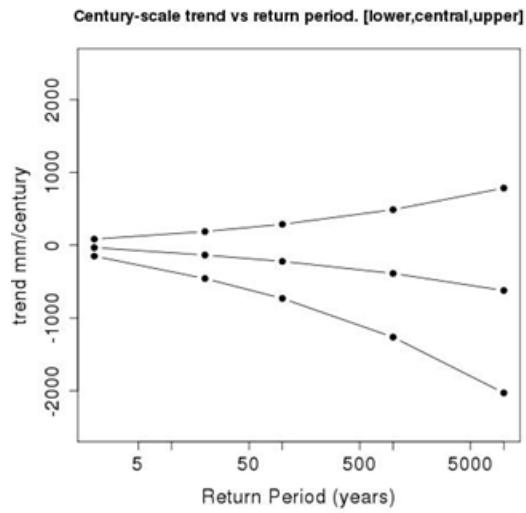


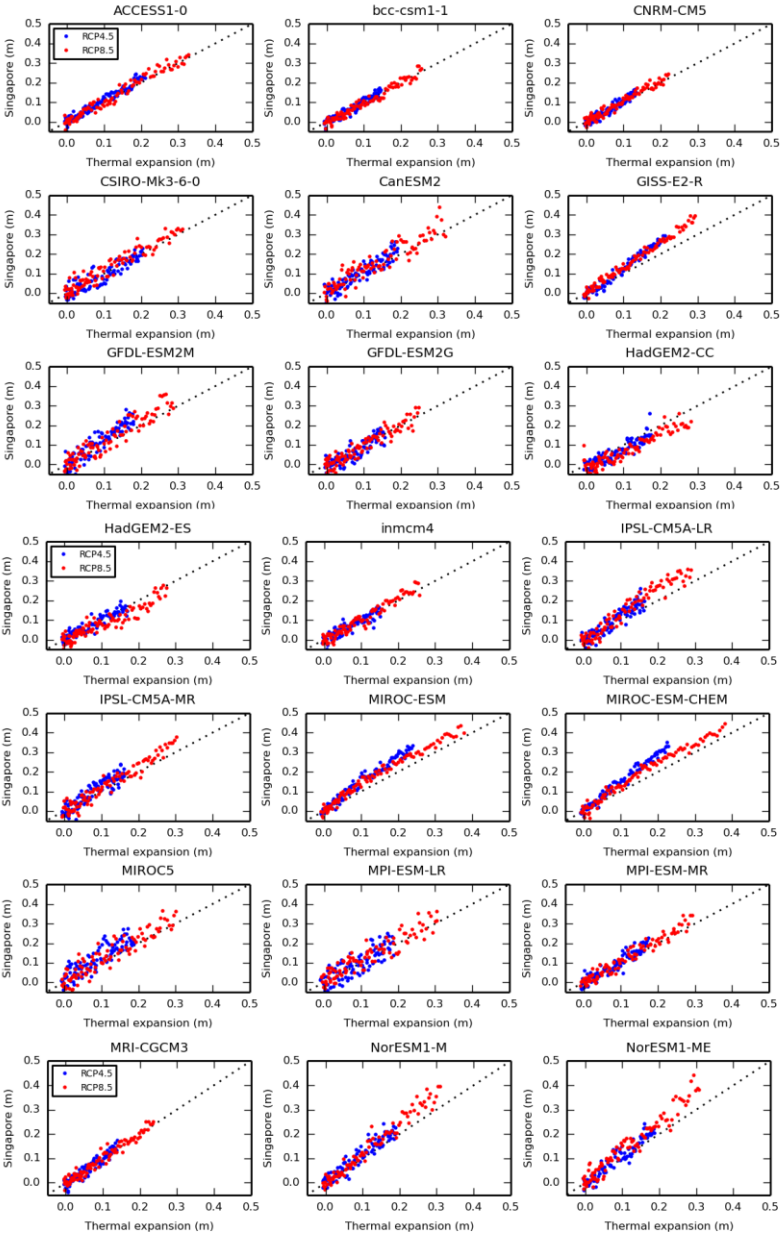
**Figure 9:** Simulated annual maxima of significant wave height (metres) obtained from the (a) GFDL, (b) HadGEM, (c) CNRM, and (d) IPSL forced simulations. The P value indicates the statistical significance of the improvement in fit when using a non-stationary GEV model: a large P value indicates little improvement; a small P value indicates significant improvement.



1184  
 1185 **Figure 10:** Projected century-scale trends in significant wave height for five return periods  
 1186 due to storminess changes only (i.e. excluding mean sea level change) (mm per century).  
 1187 Central, lower and upper estimates are shown.

1188  
 1189  
 1190  
 1191  
 1192  
 1193  
 1194  
 1195  
 1196  
 1197  
 1198  
 1199





Formatted: Font: 14 pt, Bold

**Figure A1:** Regression between local oceanographic sea level change (due to steric plus dynamic processes) and global thermal expansion terms for each CMIP5 model under RCP 4.5 and RCP 8.5.

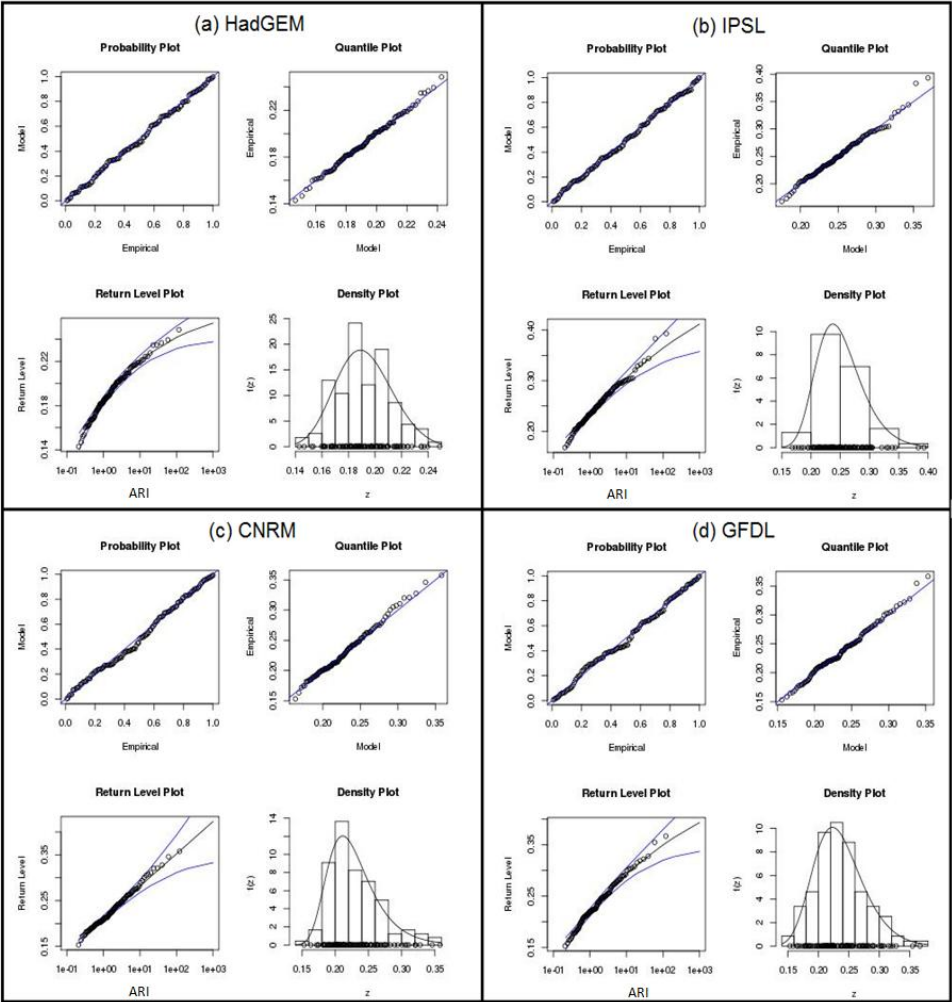


**Figure A21:** Standard diagnostic plots for stationary fit to skew surge annual maxima from (a) HadGEM2-ES, (b) IPSL, (c) CNRM, and (d) GFDL simulations. The quantile and probability plots compare the theoretical distribution fitted to the data with the actual data and give an indication of confidence in the fit of the return period.

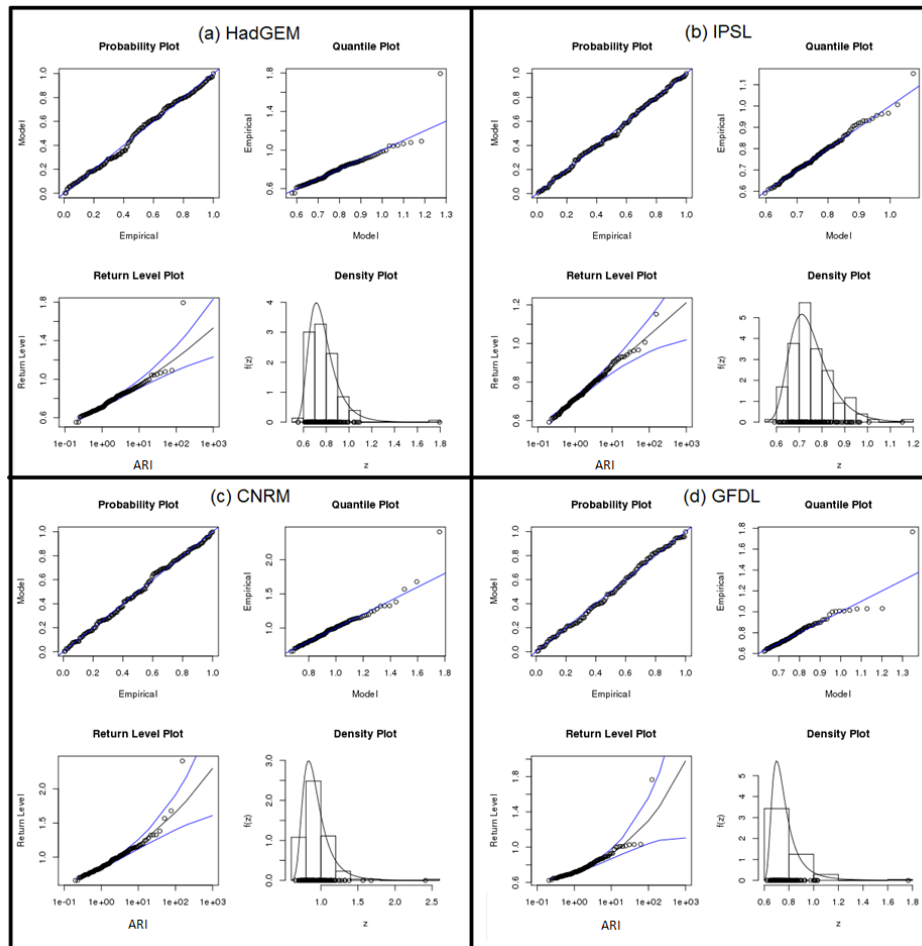


**Figure A32:** Standard diagnostic plots for stationary fit to significant wave height annual maxima from (a) HadGEM2-ES, (b) IPSL, (c) CNRM and (d) GFDL simulations. The quantile and probability plots compare the theoretical distribution fitted to the data with the actual data and give an indication of confidence in the fit of the return period.